Endocytosis of EGFR requires its kinase activity and N-terminal transmembrane dimerization motif

Raimond Heukers[1], Jeroen F. Vermeulen[1], Farzad Fereidouni[2], Arjen N. Bader[2,*], Jarno Voortman[1], Rob C. Roovers[1,‡], Hans C. Gerritsen[2] and Paul M. P. van Bergen en Henegouwen[1,§]

[1]Cell Biology, Department of Biology, Science Faculty, Utrecht University, 3584 CH Utrecht, The Netherlands
[2]Molecular Biophysics, Science Faculty, Utrecht University, 3584 CH Utrecht, The Netherlands

*Present address: Wageningen University, 6703 HA Wageningen, The Netherlands
‡Present address: Merus Biopharmaceuticals, 3584 CH Utrecht, The Netherlands
§Author for correspondence (p.vanbergen@uu.nl)

Accepted 31 July 2013
Journal of Cell Science 126, 4900–4912

doi: 10.1242/jcs.128611

Summary

EGFR signaling is attenuated by endocytosis and degradation of receptor–ligand complexes in lysosomes. Endocytosis of EGFR is known to be regulated by multiple post-translational modifications. The observation that prevention of these modifications does not block endocytosis completely, suggests the involvement of other mechanism(s). Recently, receptor clustering has been suggested to induce internalization of multiple types of membrane receptors. However, the mechanism of clustering-induced internalization remains unknown. We have used biparatopic antibody fragments from llama (VHHs) to induce EGFR clustering without stimulating tyrosine kinase activity. Using this approach, we have found an essential role for the N-terminal GG4-like dimerization motif in the transmembrane domain (TMD) for clustering-induced internalization. Moreover, conventional EGF-induced receptor internalization depends exclusively on this TMD dimerization and kinase activity. Mutations in this dimerization motif eventually lead to reduced EGFR degradation and sustained signaling. We propose a novel role for the TMD dimerization motif in the negative-feedback control of EGFR. The widely conserved nature of GG4-like dimerization motifs in transmembrane proteins suggests a general role for these motifs in clustering-induced internalization.

Key words: Clustering, EGFR endocytosis, Transmembrane domain, VHH, Nanobody

Introduction

The receptor for the epidermal growth factor (EGFR, HER1 or ErbB1) is a receptor tyrosine kinase that, together with its family members HER2, HER3 and HER4, belongs to the ErbB family of growth factor receptors (Yarden, 2001). This family of receptor tyrosine kinases is involved in the growth regulation of many different cancers, such as brain, breast, and head and neck tumors. In resting cells, the different members of the ErbB family are present in the plasma membrane as inactive monomers or as inactive homo- and hetero-dimers (predimers). EGF binding induces the formation of additional dimers, tetramers and further higher-order oligomers (Clayton et al., 2005; Clayton et al., 2007; Clayton et al., 2008; Hofman et al., 2010; Saffarian et al., 2007; Whitson et al., 2004). In addition, EGF initiates several structural rearrangements in the ecto- and intracellular domain, which releases its auto-inhibition, resulting in kinase activation and trans-phosphorylation of C-terminal tyrosine residues (Jura et al., 2009; Thiel and Carpenter, 2007). The phosphorylated tyrosines serve subsequently as docking sites for various adaptor proteins involved in signal transduction of proliferative and anti-apoptotic pathways (Burgess, 2008; Citri and Yarden, 2006).

The ErbB receptors are all composed of similar building blocks such as the extracellular domain, which comprises subdomains I–IV, the trans- and juxtamembrane domains, the tyrosine kinase and the substrate domain (Burgess, 2008). The structural interactions required for receptor oligomerization are less well described but crystal data from ectodomains with bound ligands show different head-to-head interactions, which might be involved in cluster formation (Clayton et al., 2008; Garrett et al., 2002; Groenen et al., 1997). Recent data also suggest a role for signaling in receptor clustering because inhibition of receptor kinase activity or phospholipase D activity prevented EGFR clustering (Ariotti et al., 2010; Clayton et al., 2007; Hofman et al., 2010). Dimerization of EGFR could also be regulated by two Sternberg–Gullick (GxxxG- or GG4-like) dimerization motifs within the transmembrane domain (TMD). Disulfide-crosslinking experiments indicated EGF-induced association of the N-terminal GG4 motif (Lu et al., 2010). Interestingly, mutations in the TMD of EGFR are frequently implicated in different types of disease (Li and Hristova, 2006).

One of the most important negative-feedback mechanisms of EGFR signaling is receptor downregulation, which is initiated by clathrin-mediated endocytosis (CME) and/or clathrin-independent endocytosis (Madshus and Stang, 2009; Sorkin and Goh, 2008). After their internalization, active receptor–ligand complexes are transported by multi-vesicular vesicles to lysosomes where the complexes are degraded (Lai et al., 1989). Ligand binding induces a large increase in the internalization rate, which is regulated at different levels (Sorkin and Goh, 2008). Although post-translational modifications such as tyrosine and serine/threonine phosphorylation, ubiquitylation and acetylation all play a role in regulating receptor endocytosis, blocking these modifications does

not inhibit EGFR internalization completely, suggesting the existence of other as yet undefined mechanisms (Goh et al., 2010; Huang et al., 2007; Wang et al., 2007). Recently, different antibody combinations or multitopic constructs showed a reduction in surface-expressed EGFR as a result of the kinase-independent internalization of EGFR, suggesting the involvement of EGFR clustering in EGFR internalization (Boersma et al., 2011; Friedman et al., 2005; Hackel et al., 2012; Spangler et al., 2010).

In this study, we have investigated the role of receptor clustering in the internalization of EGFR by using biparatopic VHHs. VHHs or nanobodies consist of the variable domain of the heavy chain from heavy-chain-only antibodies from *Llama glama* (Muyldermans et al., 1994; Roovers et al., 2007b; Van Bockstaele et al., 2009). Biparatopic VHHs are bivalent anti-EGFR VHHs that are binding to two different, non-overlapping epitopes on the extracellular domain of EGFR (Roovers et al., 2011; Schmitz et al., 2013). Anisotropy studies presented here show that biparatopic VHHs stimulate EGFR clustering to a similar extent as EGF without stimulating kinase activity. Clustering-induced internalization of EGFR was clathrin-mediated and depended entirely on its N-terminal TMD dimerization motif. Moreover, EGF-induced internalization of EGFR was completely blocked by a mutation in the N-terminal TMD dimerization motif in combination with a mutation inactivating the kinase. Mutations in the TMD reduced EGF-induced degradation of both EGFR and EGF, resulting in sustained signaling. We propose a model in which ligand-induced CME is regulated by receptor clustering in synergy with adaptor proteins that are recruited to the post-translationally modified EGFR C-terminal tail.

Results

Generation and characterization of biparatopic VHHs against the EGFR ectodomain

To study the role of receptor clustering in EGFR internalization we aimed to induce receptor clustering by using biparatopic nanobodies that bind intermolecularly to EGFRs without stimulating kinase activity. Different anti-EGFR VHH constructs were used (Mono1–Mono4) as building blocks for the biparatopic nanobodies (Fig. 1A). The selection of the antagonistic monomeric VHHs 7D12 (Mono1) and 9G8 (Mono2) was previously described (Roovers et al., 2011). These nanobodies bind to domain III, compete for EGF binding and in addition, compete for binding of either cetuximab (7D12) or matuzumab (9G8). In another biparatopic construct, two non-EGF competing anti-EGFR nanobodies were used: the previously described EGb4 (Mono3) (Hofman et al., 2008) and EGc9 (Mono4). The latter VHH was obtained from a new selection performed on bacterially expressed, recombinant EGFR domain I. Binding of these VHHs to recombinant EGFR ectodomain was shown by phage ELISA. As a negative control, a phage expressing a non-relevant VHH (NR-VHH) was used, which did not show any binding (Fig. 1B). A phage ELISA was also used to demonstrate binding of Mono3 and Mono4 to EGFR domain I (Fig. 1C).

From these four building blocks, two biparatopic VHHs were generated, of which the different VHH building blocks bind to non-overlapping epitopes on the ectodomain (Fig. 1A). To demonstrate this, cross-competition studies with monovalent VHHs and VHH-expressing phages were performed. Mono2-expressing phages were successfully displaced by a 100-fold excess of Mono2 protein, whereas binding was unaffected by the presence of a 100-fold excess of Mono1 (Fig. 1D, left). In a similar experiment, we showed that Mono3 and Mono4 also bind to non-overlapping epitopes (Fig. 1D, right). These monovalent VHHs were subsequently fused to form the bivalent, mono-specific Bival1 (Mono1–Mono1), biparatopic Bipar1 (Mono1–Mono2) or biparatopic Bipar2 (Mono2–Mono3) using a 10-residue glycine-serine linker (Fig. 1A). A cross-competition assay with HER14 cells showed that the two biparatopic VHHs do not compete with each other for EGFR binding (Fig. 1E). Recent X-ray data with Mono1 and Mono2 (7D12 and 9G8) showed that the 10-residue linker is too short for intramolecular binding of the two epitope-binding domains to a single EGFR (Schmitz et al., 2013). In agreement with this is the result obtained with a sedimentation velocity analytical ultracentrifugation (SV-AUC) experiment where Bipar1 binds EGFR with a 1:2 (VHH:EGFR) stoichiometry (Schmitz et al., 2013). This intermolecular binding would enable Bipar1 to stimulate higher-order EGFR clusters on cells.

Because activation of EGFR is accompanied with EGFR oligomerization, we first checked whether the biparatopic VHHs are non-agonistic. Whereas EGF treatment resulted in a clear phosphorylation of EGFR, the VHH constructs lacked agonistic activity (Fig. 1F). In conclusion, we have generated two non-agonistic biparatopic VHHs, which both consist of two non-overlapping epitope-binding nanobodies: one that interacts with domain III (Bipar1) and the other with domain I (Bipar2).

Biparatopic VHHs induce EGFR clustering

To investigate whether the anti-EGFR VHHs induce receptor clustering, we have used homo-Förster resonance energy transfer (homo-FRET) (Bader et al., 2011). In this assay, clustering of EGFR is analyzed on NIH 3T3 cells expressing EGFR fused to monomeric GFP (mGFP) by confocal time-resolved fluorescence anisotropy imaging microscopy. Homo-FRET between EGFR-mGFP molecules causes a reduction in fluorescence anisotropy, which is used as a measure for EGFR clustering (Fig. 2). Both biparatopic VHHs are able to induce similar changes in anisotropy to EGF, indicating that biparatopic VHHs generate higher-order clusters of EGFR similar to EGF (Fig. 2A). In contrast to biparatopic VHHs, binding of either monovalent or bivalent VHHs does not induce EGFR clustering (Fig. 2A). This VHH-induced clustering of EGFR was concentration dependent (Fig. 2B). Moreover, Bipar1-induced receptor clustering was lost upon addition of a 100-fold molar excess of either one of the two monovalent VHHs, Mono1 or Mono2 (Fig. 2C), demonstrating the importance of the binding of both EGFR-binding domains for EGFR clustering.

Clustering VHHs induce EGFR internalization

Because the biparatopic VHHs were shown to induce receptor clustering, they were subsequently tested for their capacity to induce receptor internalization. Internalization rate constants (k_e) were determined following a previously described method (Wiley and Cunningham, 1982). Uptake of non-agonistic monovalent VHHs is considered as pinocytosis (k_e=0.0025 minute^{-1}). Activation of EGFR by EGF stimulates internalization up to 40 times (k_e=0.14 minute^{-1}) compared with the pinocytosis (Fig. 3A).

The bivalent monospecific VHHs stimulated EGFR internalization slightly (Fig. 3B). However, a threefold increase in EGFR internalization was observed with the biparatopic construct ($k_{e,mono}$=0.003 minute^{-1}, $k_{e,bivalent}$=0.005 minute^{-1}

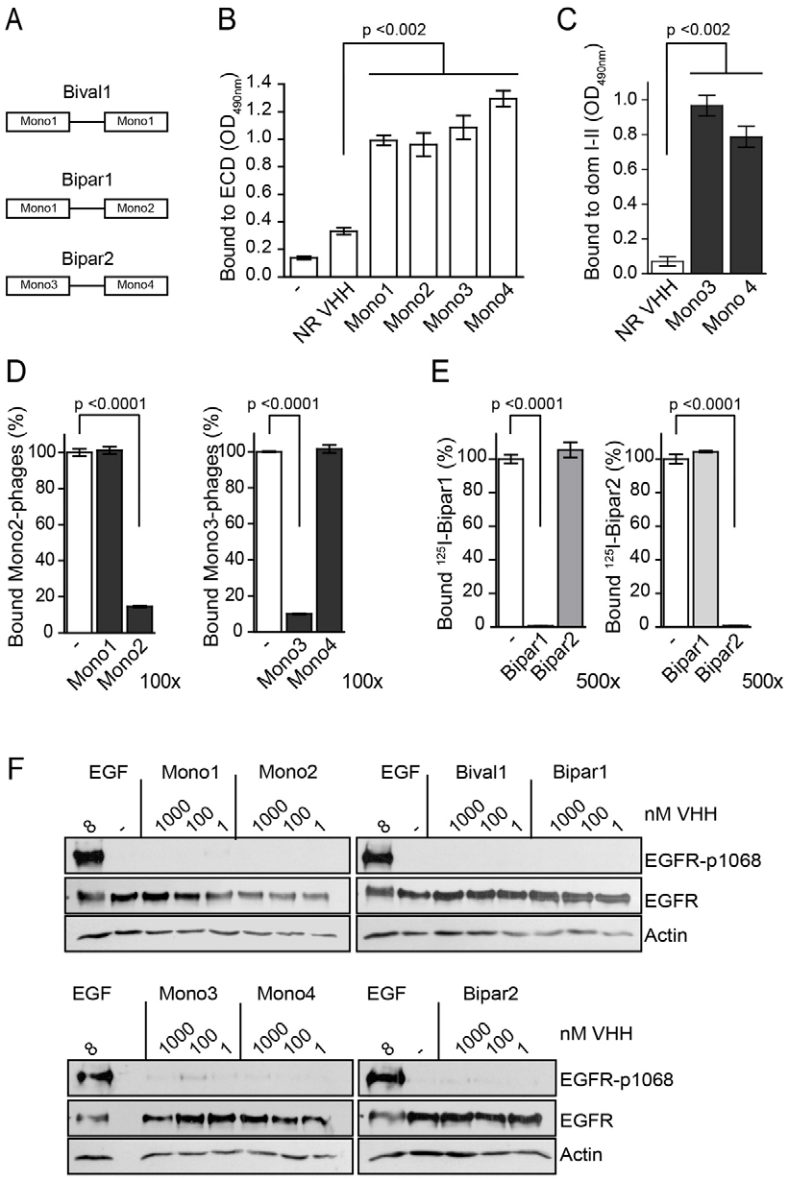

Fig. 1. Selected VHHs bind at non-overlapping sites on the EGFR ectodomain. (A) Schematic presentation of nanobody constructs. Phages expressing the indicated VHHs or a non-relevant VHH were bound to the EGFR extracellular domain (B) or domain I+II of the EGFR extracellular domain (C) for 1 hour at room temperature. Bound phages were detected by ELISA with anti-M13 antibodies and OPD/H_2O_2. (D) Cross-competition of phages expressing Mono2 or Mono3 for binding to EGFR extracellular domain with an excess of indicated VHHs. Bound phages were detected as indicated in A. (E) Cross-competition of ^{125}I-labeled Bipar1 (left) or Bipar2 (right) by 500-fold molar excess of unlabeled VHHs on HER14 cells. Cells were incubated with VHHs for 2 hours on ice, after which radioactivity was quantified. (F) HER14 cells were serum starved for 4 hours and treated for 10 minutes with either 8 nM of EGF or a concentration range of VHHs. Phosphorylated EGFR and total EGFR was detected on blots using anti-pEGFR (pY1068) and anti-EGFR antibodies. Actin was used as loading control. Error bars represent s.e.m.

and $k_{e,Bipar1}$=0.009 minute^{-1}) (Fig. 3B). Although directed against different epitopes, both biparatopic VHHs internalized at a similar internalization rate. Since the two biparatopic VHHs bind non-overlapping epitopes themselves, we aimed for even faster internalization by treatment of cells with Bipar1 and Bipar2 simultaneously. This combination did not significantly enhance the internalization rate compared with biparatopic VHHs alone (k_e=0.011 minute^{-1}, Fig. 3B). Furthermore, internalization rate constants of Bipar1 were concentration dependent up to 50 nM, resulting in a maximum internalization rate constant of 0.013 minute^{-1} (Fig. 3C). This is a more than fourfold increase in internalization compared with pinocytosis. Excess of either Mono1 or Mono2, which prevented clustering, similarly reduced the internalization rate constant of Bipar1 back to that of pinocytosis (Fig. 3D). This observation demonstrates that the intermolecular interactions of biparatopic VHHs are essential for biparatopic VHH-induced EGFR internalization. Moreover, rate constants of Bipar1-induced internalization were similar for cells expressing different levels of EGFR: for high EGFR expression levels, we used A431 [2.6×10^6 receptors/cell (Haigler et al., 1978)], for moderate expression levels, UM-SCC-14C and HER14 cells [3×10^5 receptors/cell (Honegger et al., 1987)] and for low expression levels, HeLa cells [5×10^4 receptors/cell (Berkers et al., 1991)]. This shows that Bipar1-induced internalization occurs irrespective of the EGFR expression level (Fig. 3E).

We so far determined internalization rate constants of the ligands. To test whether the internalization rate constants determined for the ligands corresponds to the rate constants of the EGFR itself, we used ^{125}I-labeled Mono3, a non-agonistic anti-EGFR VHH that does not compete with the binding of EGF or Bipar1. Treatment with 10 nM of unlabeled Bipar1 did indeed induce internalization of EGb4 at a similar rate as the ^{125}I-labeled biparatopic VHHs (Fig. 3F). This suggests that the measured internalization rate constant of Bipar-1 reflects the internalization rate of the receptor itself. Taken together, these data demonstrate that extracellular clustering of EGFR by biparatopic VHHs stimulates EGFR internalization levels up to four times compared

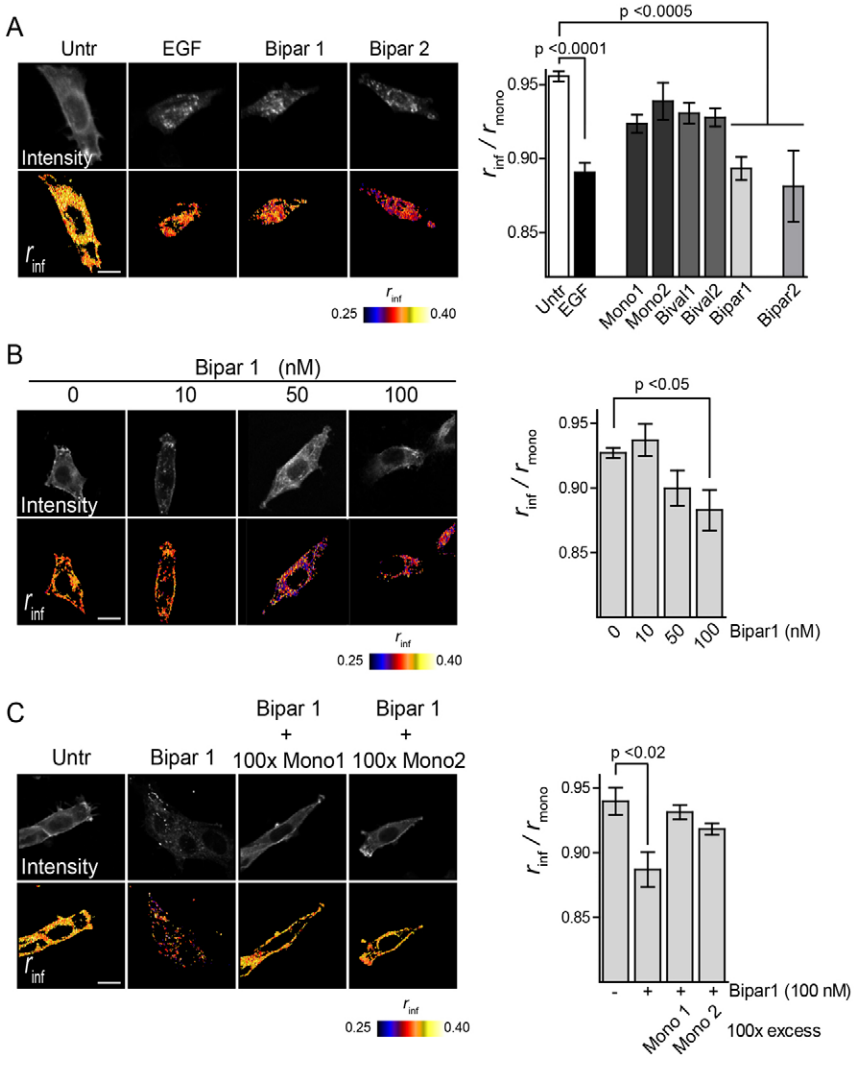

Fig. 2. Biparatopic VHHs cluster EGFR to same extent as EGF. (A) Confocal time-resolved fluorescence anisotropy imaging microscopy (CTR-FAIM) analysis of receptor clustering. NIH 3T3 2.2 cells expressing EGFR-mGFP were seeded on glass coverslips and allowed to adhere overnight. Cells were treated with 50 nM of the indicated VHHs for 20 minutes or 8 nM of EGF for 10 minutes at 37℃ and subsequently fixed. Changes in anisotropy values, as a result of homo-FRET, were determined as described in the Materials and Methods and presented in false colors. Limiting anisotropy values (r_{inf}) of EGFR-mGFP were plotted as fraction of the anisotropy value of mGFP (r_{mono}). (B) Bipar1-induced EGFR clustering is concentration dependent. EGFR-mGFP-expressing cells were treated with indicated concentrations of Bipar1 for 20 minutes and anisotropy values were determined. (**C**) VHH-induced clustering of EGFR depends on binding of both epitope-binding domains. EGFR-mGFP-expressing cells were treated with 100 nM Bipar1 with or without a 100-fold excess or either Mono1 or Mono2 for 20 minutes and anisotropy values were determined. Scale bars: 20 μm. Error bars represent s.e.m. with $n>5$.

with pinocytosis. This effect was seen regardless the binding specificity of the two biparatopic VHHs.

Clustering-induced internalization occurs by clathrin-mediated endocytosis

EGF-induced endocytosis of EGFR occurs through clathrin-mediated and clathrin-independent pathways. To determine which of these pathways is used by VHH-induced EGFR internalization, we analyzed whether we could detect any colocalization of EGFR with clathrin on the cell membrane by live-cell dual-color total internal reflection fluorescence microscopy (TIRFM). Therefore, Bipar1 or EGF was labeled with Alexa Fluor 488 and applied to HER14 cells expressing RFP-clathrin. After addition of fluorescent ligand, internalization was monitored for several minutes (Fig. 4A, top; supplementary material Figs S1,S2 and Movies 1,2). EGF clusters internalized through pre-existing clathrin-coated lattices or sheets, which is in agreement with a previous publication (Rappoport and Simon, 2009). The Bipar1-induced EGFR clusters also internalized through pre-existing clathrin sheets. Furthermore, at the onset of colocalization with pre-existing clathrin-coated sheets, a dynamic reorganization and accumulation of clathrin was observed (supplementary material Movie 2). These data show that EGFR clusters accumulate at pre-existing clathrin-coated sheets where coated pits and vesicles are formed and then pinch off from the plasma membrane.

More evidence for a role of CME in clustering-induced internalization of EGFR was obtained by overexpression of a dominant-negative version of Eps15 lacking the EH domains (Eps15ΔI). This mutant is unable to bind EGFR and instead blocks clathrin-mediated endocytosis by sequestering AP2 and CHC (Benmerah et al., 1999). Overexpression of Eps15ΔI strongly inhibited Bipar1 internalization, but had no effect on internalization of EGF (Fig. 4B). This indicates that Bipar1-induced internalization completely depends on the clathrin-mediated route, whereas an alternative clathrin-independent route exists for EGF (Huang et al., 2004; Sigismund et al., 2005). To obtain more evidence for the clathrin dependence of Bipar-induced EGFR internalization, we blocked CME by inhibiting phosphatidylinositol 4,5-bisphosphate (PIP2) production with primary alcohols (Boucrot et al., 2006). PIP2 recruits various adaptor proteins of the CME machinery. Internalization of Bipar1, transferrin (Trf) and cholera toxin B (CTB) was assessed in the presence of the primary alcohol 1-butanol. Although the clathrin-mediated uptake of both Bipar1 and Trf was blocked, CTB was internalized normally (supplementary

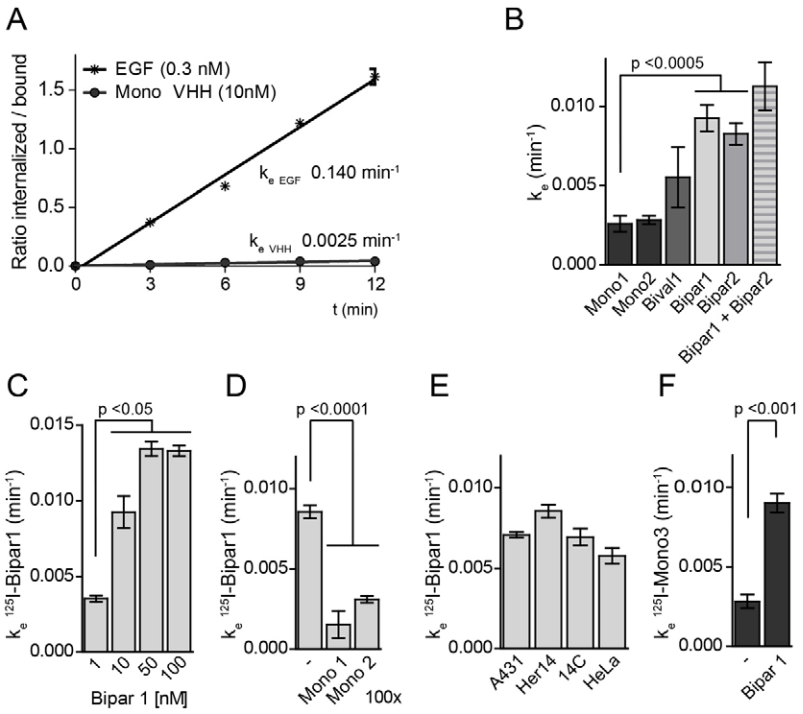

Fig. 3. EGFR clustering by biparatopic VHHs induces internalization of both receptor and VHH. (A) EGF induces rapid EGFR internalization. 10 nM of ^{125}I-labeled monovalent VHH or 0.3 nM of EGF was allowed to internalize for 3, 6, 9 and 12 minutes. Cells were stripped (bound fraction) and lysed in 1 M NaOH (internalized fraction). Internalized/bound fractions were plotted in time. This data was used to determine the internalization rate constants (k_e). (B) Biparatopic VHHs internalize faster than monovalent ones. 10 nM of ^{125}I-labeled VHHs were allowed to internalize into HER14 cells for up to 12 minutes. For treatment with Bipar1 and Bipar2, a mixture of 10 nM unlabeled Bipar2 and 10 nM ^{125}I-labeled Bipar1 was used. (C) Bipar1-induced internalization rate is concentration dependent up to 50 nM. (D) Induction of internalization by biparatopic VHHs requires both EGFR binding domains. Internalization rate constants of ^{125}I-labeled Bipar1 were determined with or without 500-fold molar excess of Mono1 or Mono2. (E) The k_e of Bipar1 is independent of EGFR expression levels. Internalization rates of 10 nM ^{125}I-labeled Bipar1 were determined in A431, HER14, 14C and HeLa cells. (F) Upon treatment with biparatopic VHHs, EGFR is internalized with a similar rate as the VHHs. The k_e of EGFR was determined with ^{125}I-EGb4 by co-incubation with 10 nM of unlabeled Mono1 or Bipar1. Error bars represent s.e.m.

material Fig. S3). By contrast, the secondary alcohol 2-propanol had no effect on the internalization of either of these ligands. Furthermore, disruption of caveolin-mediated endocytosis by fillipin, completely inhibited CTB uptake, but had no effect on endocytosis of both Bipar1 and Trf, which excludes a role for caveolin in clustering-induced EGFR endocytosis (supplementary material Fig. S3).

The involvement of clathrin in the Bipar-induced EGFR internalization was furthermore checked by siRNA knockdown of clathrin heavy chain (CHC), the α-subunit of adaptor protein-2 (AP2) complex and Eps15. Knockdown efficiency was determined by western blotting (Fig. 4C). Knockdown of CHC reduced the internalization of Bipar1 to the level of a monovalent VHH but it did not affect internalization of monovalent VHH (Fig. 4D). Furthermore, siRNA knockdown of the α-subunit of AP2 also significantly reduced the internalization rate constant of Bipar1. However, knockdown of Eps15 had no effect on Bipar1 internalization, which was expected because Eps15 is involved in the ubiquitin-regulated endocytosis of EGFR (Sigismund et al., 2005). Finally, treatment of the cells with 80 nM Dynasore, a dynamin inhibitor, also significantly inhibited the internalization of Bipar1 (Fig. 4D) (Kirchhausen et al., 2008). This was confirmed by determining the internalization rate constant of Bipar1 and immunofluorescence studies of Bipar1in HeLa cells stably expressing the thermosensitive mutant of dynamin, Dyn-K44A (Altschuler et al., 1998) (Fig. 4E,F). Taken together, our experiments show that the clustering-induced internalization of EGFR occurs through the clathrin-, AP2- and dynamin-mediated internalization route. This phenomenon is referred to as clustering-induced clathrin-mediated endocytosis (CIC-ME).

The intracellular domain is not required for clustering-induced internalization

Activated EGFRs interact directly and indirectly with the different adaptor proteins of the CME pathway through their phosphorylated tyrosines, ubiquitylated or acetylated lysines, or other specific docking sites. Because the VHHs are not agonistic, it is unlikely that clustering-induced internalization of EGFR is dependent on kinase activity or phospho-tyrosines in the intracellular domain. To test this, internalization of Bipar1 was analyzed in NIH 3T3 2.2 cells stably expressing an EGFR mutant with an inactive tyrosine kinase domain (EGFR-K721A), or with a mutant lacking nine (phospho) tyrosine kinase substrate residues in the C-terminal tail (EGFR 9YF) (Fig. 4G). The internalization rate constants of Bipar1 in cells stably expressing these mutants were similar to those observed in cells expressing wild-type EGFR, indicating that clustering-induced internalization of EGFR is independent of its kinase activity.

Besides the phospho-tyrosine-mediated interactions, the AP2 complex can also bind to EGFR directly through two AP2-binding domains: a double leucine motif (LL1010/1011) and a tyrosine-based motif at position 974 (YRAL) (Huang et al., 2003). To determine whether Bipar-induced CME depends on these AP2-binding domains we tested CME of EGFR mutated at these sites. Bipar1 was still internalized in NIH 3T3 2.2 cells expressing either EGFR LL/AA or the double EGFR LL/AA-Y974F mutant (Fig. 4H). More surprisingly, Bipar1 was even internalized in cells expressing a mutant that lacked almost the complete intracellular part of EGFR (EGFR 1–653, Fig. 4I). No change in uptake of Mono1 was observed, indicating that the pinocytosis was not affected. Taken together, these experiments show that clustering-induced CME of EGFR does not require its intracellular domain for internalization.

Transmembrane GG4 dimerization motif is crucial for clustering-induced endocytosis

The observations that clustering-induced internalization is independent of the intracellular part of EGFR might indicate a possible role for the transmembrane domain (TMD). To test this hypothesis, we replaced the complete TMD of EGFR with a leucine-alanine repeat (EGFR-LALA) that favors an α-helical

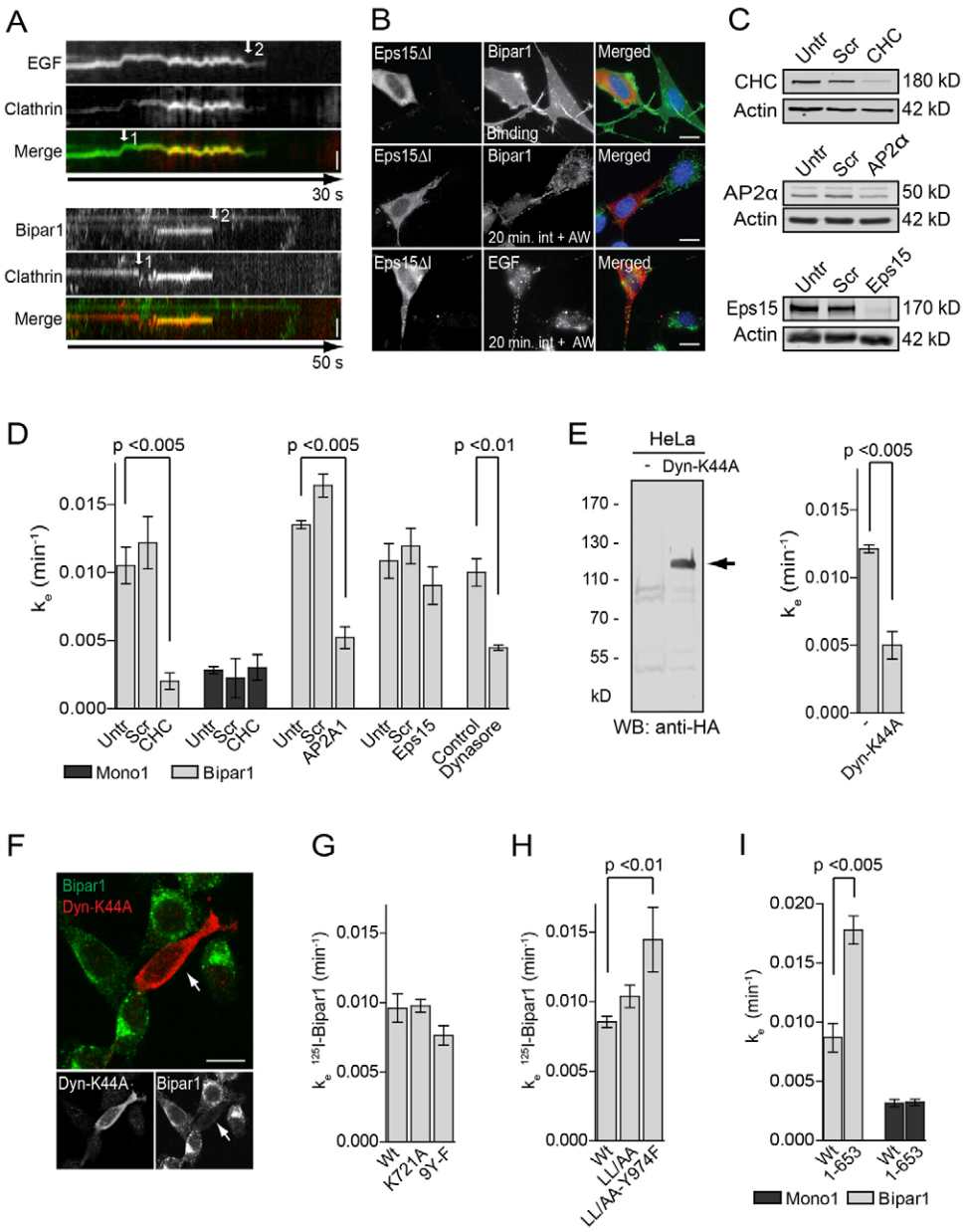

Fig. 4. Clustering-induced EGFR internalization occurs by clathrin-dependent endocytosis. (A) Live-cell, dual-color TIRF-M shows colocalization (arrow 1) of internalizing EGFR clusters (arrow 2) with dynamic clathrin-coated pits. Internalization of either EGF^{Alexa488} or Bipar1^{Alexa488} was assessed in HER14 cells expressing mRFP-Clathrin. Movies were collected in TIRF mode for 50 seconds at 10 frames/second. Scale bars: 1 µm. (B) Clustering-induced internalization is inhibited by overexpression of Eps15-ΔI. 10 nM of Bipar1^{Alexa488} or 40 nM of EGF^{Alexa488} was allowed to internalize for 20 minutes at 37°C in HER14 cells overexpressing FLAG-tagged Eps15-ΔI. Cells were stripped and permeabilized with saponin. Eps15-ΔI was detected with anti-FLAG and Alexa-Fluor-555-coupled secondary antibodies. Scale bars: 15 µm. (C,D) Clustering-induced internalization is dependent on clathrin, AP2 and dynamin. HER14 cells were left untreated or were transfected with scrambled siRNA or siRNA against CHC, AP2α or Eps15. (C) Knockdown efficiency was assessed by western blotting and actin was used as loading control. (D) The k_e of [^{125}I]Mono1 or [^{125}I]Bipar1 was determined in siRNA-treated cells described in C. To test the role of dynamin, k_e of Bipar1 was determined in HER14 cells pretreated for 30 minutes with 80 µM Dynasore or DMSO. (E) Internalization rate constant of Bipar1 was determined in HeLa cells overexpressing dynamin-K44A mutant (right). Expression of dynamin-K44A was checked by western blotting (left). The overexpression of dynamin-K44A is indicated with an arrow. (F) Internalization of Bipar1^{Alexa488} in cells expressing dynamin-K44A (arrow). Cells were treated as in B, and dynamin-K44A was detected with anti-HA antibodies (red). Scale bar: 15 µm. (G–I) The k_e of Bipar1 was determined in NIH-3T3 2.2 cells stably expressing the kinase-dead mutant (K721A), a mutant in which nine phospho-tyrosines were mutated into phenylalanines (9Y-F) (G), mutants lacking either one (EGFR-LL/AA) or both (EGFR-LL/AA-Y974F) AP2-binding domains (H) or a mutant lacking the complete intracellular part (EGFR 1–653) (I). Error bars represent s.e.m.

conformation (Fig. 5A,B). In cells stably expressing the EGFR-LALA mutant, the internalization rate of Bipar1 was reduced back to that of pinocytosis (Fig. 5C). By contrast, pinocytosis, as measured with Mono1, remained unchanged. This indicates that the TMD is indeed essential for regulating clustering-induced endocytosis.

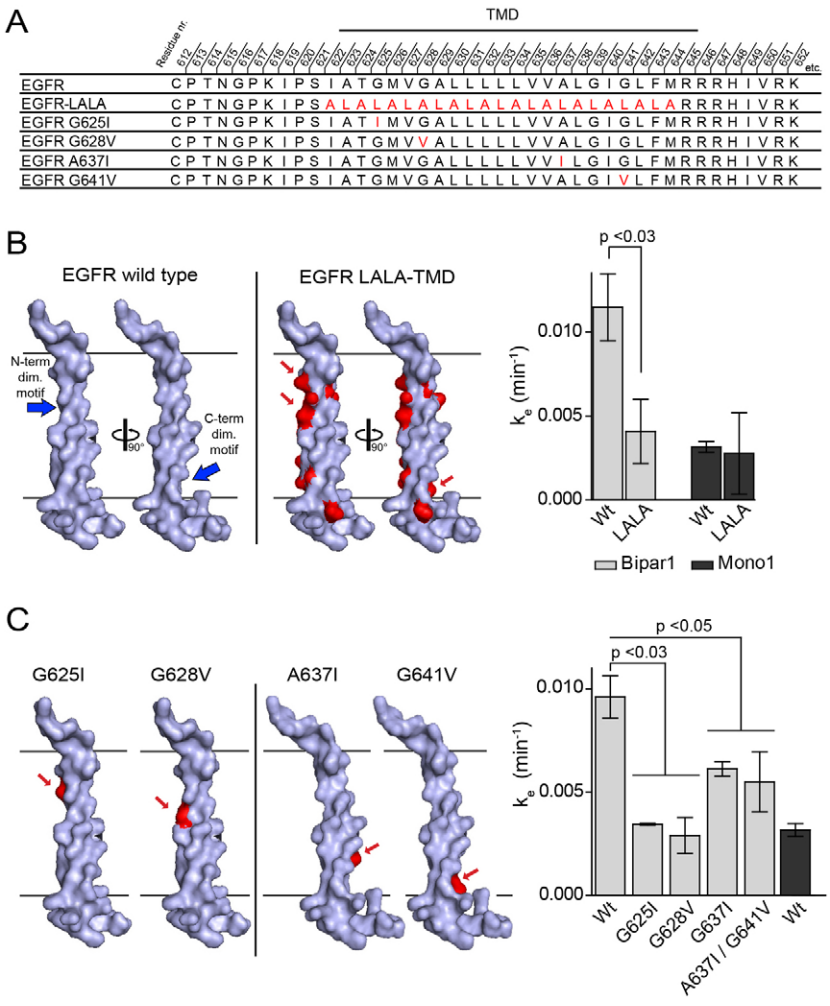

Fig. 5. Clustering-induced endocytosis is regulated by the N-terminal TMD-dimerization motif. (A) TMD and flanking sequences of EGFR and its LALA (TMD of a leucine-alanine repeat), G625I (numbering is excluding signal sequence), G628V, A637I and G641V mutants. Mutated residues are indicated in red. (B) Model of the TMD of EGFR and the LALA mutant (left). The blue arrows indicate the N-terminal and C-terminal GG4 dimerization motifs. The red arrows indicate the mutated residues (red) that fill up this groove. Domain structures were modeled using SWISS-MODEL automated homology-based modeling and PyMOL. The k_e of Mono1 or Bipar1 was determined in NIH-3T3 2.2 cells stably expressing wild-type EGFR or its LALA mutant (right). (C) Models of EGFR TMDs containing the G625I, G628V, G637I and G641V mutations (left). The k_e of Mono1 or Bipar1 was determined in NIH-3T3 2.2 cells stably expressing wild-type EGFR or the G625I, G628V, A637I and A637I/G641V mutants (right). Error bars represent s.e.m.

ErbB receptors have two (small)xxx(small) motifs (also called Sternberg–Gullick, GxxxG or GG4 motifs) in their TMD, indicated as the N-terminal or C-terminal TMD-dimerization motif. Such motifs form a ‘groove’, which stabilizes TMD dimers by forming a well-packed interface through van der Waals interactions (MacKenzie et al., 1997). To investigate the role for the N-terminal TMD-dimerization motif in clustering-induced EGFR internalization, we replaced the two small residues (glycines) in this motif with either isoleucine (G625I) or valine (G628V) (Fig. 5A,C). Both mutations were described previously to disrupt the dimerization of TMDs (Escher et al., 2009; Mendrola et al., 2002). To test whether the C-terminal TMD-dimerization motif is also involved in this internalization, this was also mutated (A637I) or valine (G641V) (Fig. 5A,C). Cell lines stably expressing these mutant EGFRs were made and sorted for similar expression levels (supplementary material Table S1). Interestingly, both TMD point mutations of the N-terminal dimerization motif completely blocked the internalization of Bipar1 (Fig. 5C). In these cells, the residual internalization rate was comparable to pinocytosis, as measured with uptake of Mono1. The C-terminal TMD mutation also affected the internalization rate of Bipar1, but not to the same extent as mutation of the N-terminal motif. Control experiments show that binding of Bipar1 to wild-type EGFR or the TMD mutants (G625I, G628V) cannot be outcompeted by the monovalent VHHs, demonstrating biparatopic binding (supplementary material Fig. S4A). Moreover, control anisotropy experiments showed that these mutants could still be clustered by either EGF or Bipar1, similar to wild-type EGFR (supplementary material Fig. S4A,B). On the basis of these results, we conclude that the TMD and more specifically, the N-terminal GG4 motif of EGFR-TMD, is crucial for clustering-induced internalization.

A role for the TMD GG4 motif in EGF-induced receptor internalization

Because single point mutations in the TMD of EGFR have such drastic effects on clustering-induced internalization, we questioned their role in EGF-induced endocytosis of EGFR. To this end, the above-described replacement of the TMD with a LALA repeat and the different point mutations were used to investigate the internalization of EGF. None of the different TMD mutations affected EGF-induced kinase activation and downstream MAPK signaling (Fig. 6A), which is in agreement with observations that the TMD is not essential for kinase activation (Lu et al., 2010). However, a significant reduction in the internalization rate constant of EGF was observed for the LALA-TMD and the G628V mutation (Fig. 6B). The effect of the G625I mutation was less severe, although still apparent and significant. By contrast, mutations in the C-terminal TMD-dimerization motif did not affect internalization at all (A637I) or

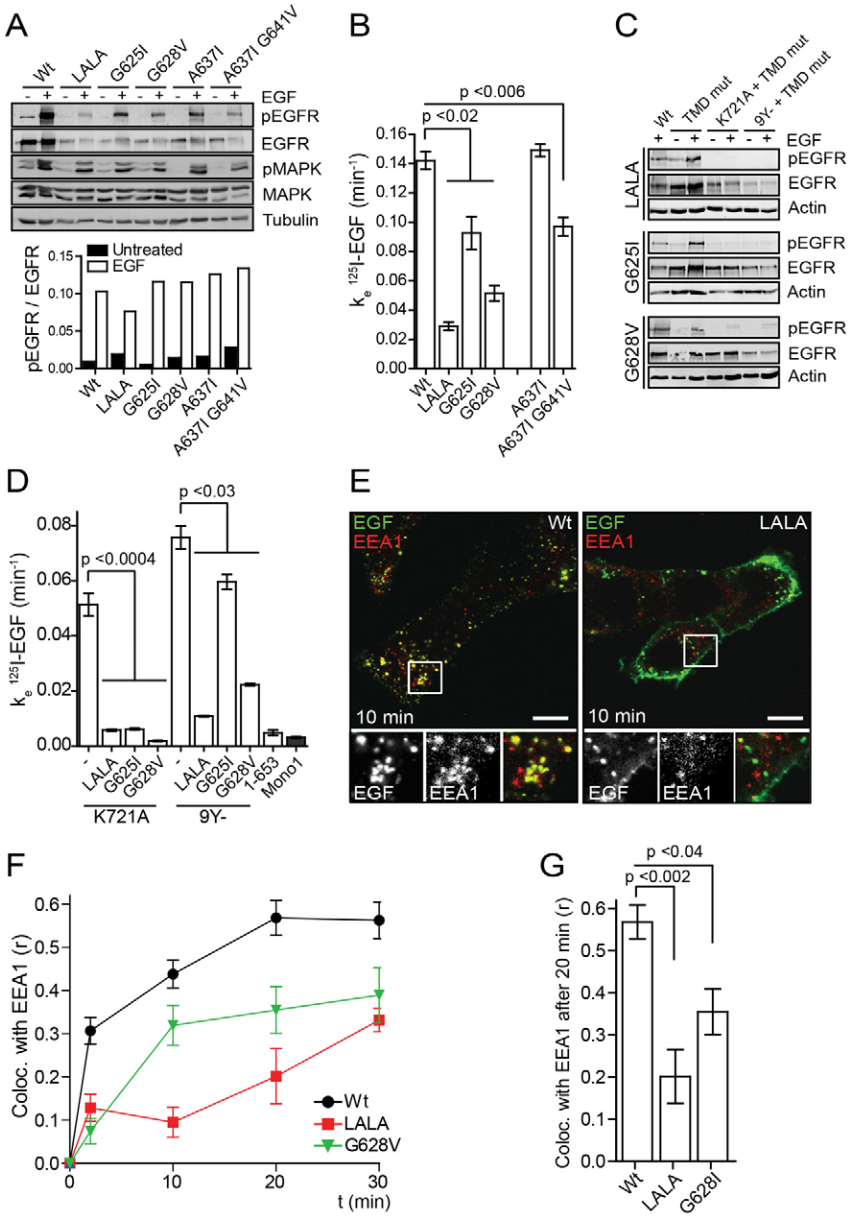

Fig. 6. Ligand-induced endocytosis is mediated by TMD dimerization and kinase activity. (A) Mutations in the TMD of EGFR do not influence EGF-induced receptor activation. NIH-3T3 2.2 cells stably expressing the indicated mutants were serum starved for 4 hours and treated with 8 nM of EGF for 10 minutes. Phosphorylated EGFR, total EGFR expression and α-tubulin was detected by western blotting. (B) EGF internalization is dependent on the N-terminal TMD dimerization motif. The k_e of 80 pM (0.5 ng/ml) of [^{125}I]EGF was determined in the cell lines shown in A. (C) Lack of kinase activity or phosphotyrosines was tested by western blotting. NIH-3T3 2.2 cells stably expressing either EGFR-K721A or EGFR-9Y-F mutants or variants containing the TMD mutations were treated as in A. (D) The k_e of 80 pM of [^{125}I]EGF was determined in the cell lines shown in C. Surface expression levels of these EGFR mutants are shown in supplementary material Table S1. (E) Colocalization of EGF^{Alexa488} with EEA1 after 10 minutes of treatment. Scale bars: 15 μm. (F) Quantification of colocalization of EGF and EEA1 in time as determined with the Pearson coefficient. (G) Quantification of colocalization of EGF and EEA1 after 20 minutes. Error bars represent s.e.m.

to a minor extent (A6371I/G641V) (Fig. 6B). These results demonstrate a prominent role for the N-terminal TMD-dimerization motif in EGF-induced EGFR internalization and a minor role for the C-terminal TMD-dimerization motif.

In contrast to the observations for clustering-induced endocytosis, alterations in the TMD dimerization motifs did not reduce EGF-induced uptake to the level of pinocytosis. This residual internalization could very well be regulated by EGF-induced kinase activation. To test this hypothesis, we introduced the same TMD mutations into the EGFR kinase-dead mutant (K721A), and into an EGFR mutant lacking nine tyrosine residues in the intracellular domain (9YF). Because the N-terminal mutations had the biggest effect on EGF internalization, only those were added to the K721A and 9YF mutants. Absence of tyrosine phosphorylation of these mutants was evident from western blotting (Fig. 6C). When the TMD-mutations were combined with a kinase-inactivating mutation (K721A), a complete block of EGF-induced internalization was observed (Fig. 6D). The TMD mutations in the 9Y-F mutant did not completely abolish the EGF-induced internalization. This was observed with both glycine mutations of the GG4 motif. The observation that the 9YF mutant was still incompletely inhibited might suggest that additional internalization signals other than phospho-tyrosine sites become activated. These findings show that EGF-induced internalization of EGFR crucially depends on both the N-terminal GG4 TMD dimerization motif and a functional kinase domain. Furthermore, we conclude that factors that are not activated by phospho-tyrosine residues are also involved in EGFR internalization.

So far, the effects of mutations in the TMD dimerization motifs were only detected within the first 12 minutes of endocytosis. To study the effects of these mutations on a longer term, localization of EGF to the early endosomes was assessed over time (Fig. 6E–G). In the case of wild-type EGFRs, EGF was clearly internalized

and mostly localized into EEA1-positive vesicles after 10 minutes (Fig. 6E). However, in cells expressing the EGFR-LALA mutant, EGF was still located on the cell surface after 10 minutes and did not colocalize with EEA1. The EGFR-LALA and EGFR-G628V mutants showed a clear delay in localization of EGF into early endosomes compared with wild-type EGFR (Fig. 6F). After 20 minutes, localization of EGF into EEA1 endosomes in significantly reduced in the EGFR-LALA and EGFR-G628V mutants compared with wild-type EGFR (Fig. 6G). Taken together, our experiments reveal a role for TMD dimerization motifs in the EGF-induced internalization of EGFR.

The N-terminal TMD dimerization motif in EGFR is required for an EGF-induced negative-feedback mechanism

To assess whether mutations in the TMD dimerization motif would also affect the EGF-induced downregulation, cells expressing either the wild type or the TMD mutants were treated for up to 8 hours with EGF. Subsequently, the effect on total EGFR levels and downstream signaling was measured (Fig. 7). In wild-type EGFR, EGF-induced activation of EGFR and downstream MAPK signaling was rapidly attenuated in time as a result of downregulation of ligand (Fig. 7E) and receptor (Fig. 7A, left panel) However, in case of the three TMD mutants, EGF-induced degradation of EGFR was significantly inhibited (Fig. 7B). More importantly, this inhibited degradation in the EGFR-LALA and G628V mutants also resulted in persistent EGFR activation and signaling towards MAPK (Fig. 7D,E). These data demonstrate that the TMD is not only important in the initial process of EGF-induced endocytosis, but also affects the subsequent events of the ligand-induced negative-feedback loop. In conclusion, our experiments reveal for the first time a role for the TMD-dimerization motifs of EGFR in ligand-induced endocytosis, and, as a consequence, also in its negative-feedback mechanism.

Discussion

Receptor downregulation is an important negative-feedback control mechanism for EGFR signaling. Mutations in EGFR that are related to an impaired downregulation are considered as hotspots in the induction of cancer (Pines et al., 2010; Polo and Di Fiore, 2006). The internalization of EGFR is regulated by multiple redundant and interdependent mechanisms (Goh et al., 2010). Binding of EGF induces several post-translational modifications of the intracellular EGFR domain, such as Ser/Thr phosphorylation, ubiquitylation and acetylation (Goh et al., 2010; Heisermann and Gill, 1988). It is not surprising that many publications have addressed the involvement of these modifications in the regulation of EGFR endocytosis. However, blocking these modifications

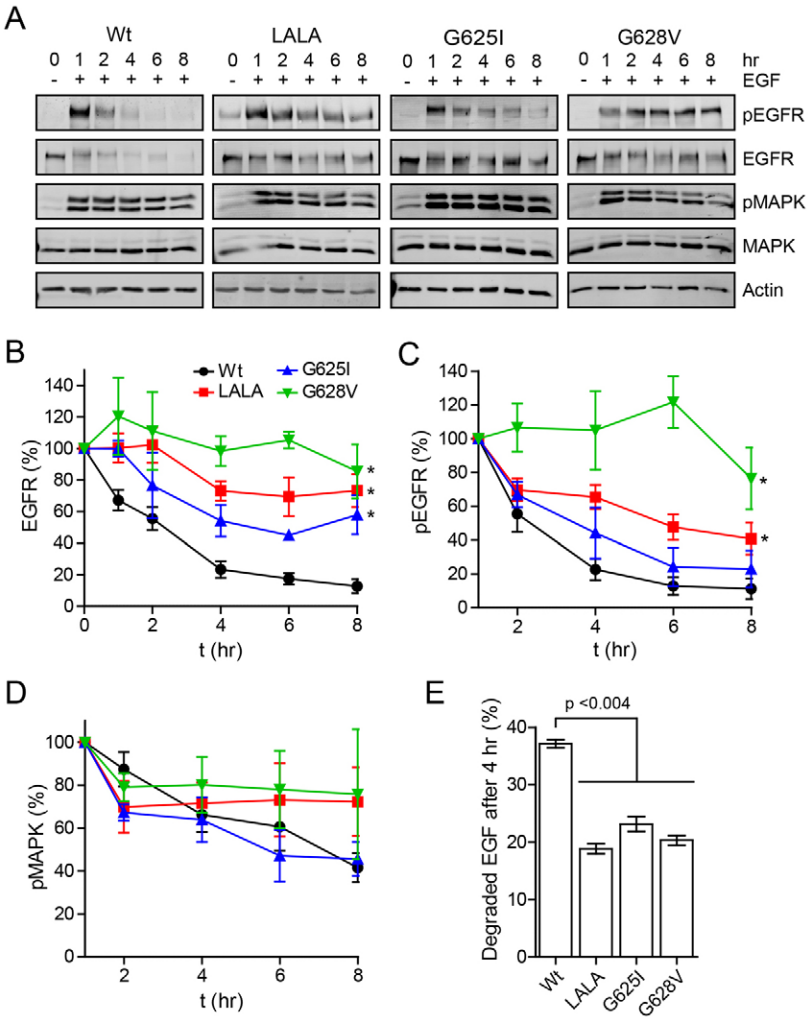

Fig. 7. Mutation of the N-terminal TMD dimerization motif affects EGFR degradation and signaling. (A) NIH-3T3 2.2 cells stably expressing the indicated mutants were serum starved for 4 hours in 0% FCS and treated with 8 nM of EGF for the indicated time periods. Phosphorylated EGFR, total EGFR, phosphorylated MAPK, MAPK and α-tubulin were detected on the blot as described in Fig. 6. (B–D) Quantification of the blots shown in A. The total EGFR (B) and phosphorylated EGFR (C) signals were corrected for equal loading as determined with α-tubulin. The signal of phosphorylated MAPK (D) was corrected for total MAPK expression. (D) EGF degradation is inhibited in the TMD mutants. ^{125}I-labeled EGF was allowed to internalize into NIH-3T3 2.2 cells stably expressing the indicated mutants for 15 minutes, after which the medium was replaced. After 4 hours, the amount of free label was measured and plotted as a percentage of the total. Error bars represent s.e.m.

never completely prevented EGFR endocytosis suggesting the existence of other mechanism(s) involved in internalization. As EGF also induces receptor clustering, we decided to investigate a possible role for receptor clustering in the internalization process by making use of the unique properties of VHHs.

By using non-agonistic, monovalent anti-EGFR VHHs (Mono1 and Mono2) we found that in resting cells, EGFR is internalized at a very low rate by pinocytosis (Fig. 3). This occurs at a rate of 0.0025 minute^{-1}, meaning that 0.25% of the initial total surface-located EGFR population is internalized per minute, requiring more than 400 minutes for a complete internalization of the initial surface-located EGFR population ($t_{½}$>200 minutes). This rate constant is much lower than the previously described fluid-phase-uptake rate of EGFR, which was determined with bivalent anti-EGFR constructs (MoAb 528) (Sunada et al., 1986; Herbst et al., 1994; Wiley et al., 1991). As shown here, receptor dimerization by bivalent constructs stimulates EGFR internalization, which could explain the higher rate of fluid phase uptake of previous studies. However, rate constants of activated EGFRs are quite similar to previously published internalization rate constants (Sorkin and Goh, 2008; Wiley 2003). As a consequence, the stimulation of internalization of active EGFRs is much larger than previously thought. Activated EGFRs are internalized at a rate >40 faster (k_e=0.10 minute^{-1}) than the pinocytosis of EGFR, and as a result, all active EGFRs are internalized within 10 minutes ($t_{½}$≈5 minutes).

By using biparatopic nanobodies we could induce EGFR clustering to a similar extent to that observed with EGF but without stimulating EGFR kinase activity (Fig. 4). Clustering of EGFR using the biparatopic nanobodies resulted in EGFR internalization with internalization rate constants that were four times higher than the pinocytosis: ~1% of surface-located EGFR was internalized per minute ($t_{½}$≈50 minutes). Interestingly, internalization rate constants of EGF-induced internalization of the kinase-dead EGFR (Fig. 6D) is still five times higher than the Bipar1-induced internalization of wild-type EGFR. Because EGF, in contrast to the VHHs, induces more than just clustering (e.g. intra- and extracellular conformational changes), other ligand-induced processes might further contribute to the observed internalization. Clustering-induced internalization was recently also observed with transferrin receptors. In that study, biotinylated receptors were expressed and extracellularly clustered using multivalent streptavidin (Liu et al., 2010). This suggests that clustering might potentially play a more general role in the internalization of transmembrane receptors.

By using several different approaches, we demonstrated that the clustering-induced internalization of EGFR occurs exclusively via the clathrin-, AP2 and dynamin-mediated pathway (Fig. 5). This is in contrast to a previous study showing that antibody-induced internalization of EGFR is not affected by clathrin knockdown (Berger et al., 2012). In this study, EGFR internalization was induced by an antibody combination of anti-EGFR (C225) and donkey-anti human IgG. This might result in the formation of very large complexes that are unable to internalize via coated vesicles. In case of Bipar1-induced internalization, deletion of the intracellular domain of EGFR revealed a function for the transmembrane domain, more particular the GG4-like dimerization motifs. This motif was first described by Sternberg and Gullick, and is present in the transmembrane domain of many growth factor receptors (Sternberg and Gullick, 1989; Sternberg and Gullick, 1990). The small residues of the GG4-like motif (blue arrows in Fig. 5) form 'grooves' that interact and stabilize TMD-dimers by Van der Waals interactions (Cymer and Schneider, 2010). Interestingly, mutations in such TMD dimerization motifs have been found in relationship with the development of different diseases (Li and Hristova, 2006). So far, the function of these GG4 motifs has been investigated in relation to receptor activation (Cymer and Schneider, 2010; Endres et al., 2013; Lu et al., 2010). However, systematic mutagenesis of this TMD, as performed in our study and in studies from others, does not indicate a role for the TMD dimerization motif in receptor activation. By contrast, a clear function for this motif was found in the clustering-induced internalization of EGFR.

Having determined a novel role for TMD dimerization motifs in clustering-induced CME, we subsequently investigated whether this motif is also involved in EGF-induced internalization. Although less complete, a clear reduction in the EGF-induced receptor internalization was observed in cells expressing EGFR with the entire TMD mutated or when either of the two glycine residues of the N-terminal motif were replaced with a larger residue (isoleucine or valine) (Fig. 6). Only one additional point mutation in the kinase domain (K721A) reduced EGF-induced receptor internalization back to the level of pinocytosis (Fig. 6). This suggests that EGFR internalization is regulated at two levels. One level involves predominantly the N-terminal dimerization motif in the TMD and the other involves its kinase activity and post-translational modifications. In the wild-type EGFR, both clustering and kinase activity might act synergistically to stimulate the uptake of EGF.

An interesting question is how these two systems cooperate in stimulating the CME of EGFR. EGFR internalization is activated by different interdependent but also redundant internalization signals (Goh et al., 2010). Following this idea, we suggest that internalization signals are already present in non-activated receptors, and can become active by receptor clustering. One of these signals might be found in the four positively charged amino acids at the C-terminal site just next to its TMD: three arginines and one histidine. Clustering of EGFR and thereby also their TMDs provides a positively charged patch just below the membrane that could function as a sink for such negatively charged lipids as phosphatidylinositol 4,5-bisphosphate (PIP_2). Several papers show the requirement for PIP_2 in the formation of the clathrin coat, for instance by binding to the AP2 subunit μ2 (Jost et al., 1998). ErbB receptors have two TMD-dimerization motifs, and bisulfide crosslinking and NMR studies showed that ErbB TMDs predominantly interact through their N-terminal GG4-like motif. Interestingly, because this dimerization occurs in an angle of 46±5°, such dimers might create a wedge-like structure in the plasma membrane (Lu et al., 2010; Mineev et al., 2010). Clustering of such wedge-like structures could potentially induce a concave membrane curvature. The observations that the N-terminal TMD-dimerization motif plays the biggest role in EGF internalization, supports this curvature hypothesis. The mechanically induced curvature can subsequently be sensed by BAR (Bin/Amphiphysin/Rvs)-domain-containing proteins. Because these proteins often contain interaction domains with CME adaptor proteins, recruitment of BAR proteins to the bent membrane domain might induce local recruitment of the CME machinery. An example of such a BAR protein is the recently identified F-BAR-domain-containing Fer/Cip4 homology domain-only proteins 1 and 2 (FCHo1/2), which has been

suggested to be involved in the initiation of EGFR internalization (Henne et al., 2010). Taken together, different mechanisms might be activated by receptor clustering, which could all contribute to the recruitment and binding of AP2 complexes, subsequently resulting in the formation of a clathrin coat. Further post-translational modifications of the EGFR intracellular domain might provide for additional interactions with components from the CME machinery, collectively contributing to the 40 times increase in EGFR internalization.

Finally, the importance of the TMD dimerization motif was demonstrated for receptor downregulation. Because this mechanism is an important feature of the negative-feedback mechanism, mutation of the dimerization domain results in sustained signaling. As such, mutations in the TMD could contribute to the malfunction of all receptors containing such TMD dimerization motifs. Several mutations have been described for the fibroblast growth factor receptor (FGFR), including a G380R mutation of FGFR3 that inhibits receptor downregulation and a G388R mutation of FGFR4, which is associated with accelerated tumor progression (Jézéquel et al., 2004; Monsonego-Ornan et al., 2000).

In summary, our experiments have demonstrated a novel role for the TMD-dimerization motif in clustering-induced receptor internalization. Because many other receptors contain such dimerization motifs, it would be interesting to investigate the role of TMD-dimerization motifs in the internalization of a broader spectrum of receptors.

Materials and Methods

Plasmids and constructs

EGFR-K721A, and EGFR-9YF, mRFP-Clathrin, Eps15-ΔI and HA-tagged Dynamin2 K44A were kindly provided by Sara Sigismund (IFOM-FIRC Institute of Molecular Oncology, Milan, Italy), Klemens Rottner (Helmholtz Centre for Infection Research, Braunschweig, Germany), Alexandre Benmerah (Institut Cochin, Paris, France) (Benmerah et al., 1999) and Sandra Schmid (Damke et al., 1994), respectively. The EGFR mutants were created by Quikchange mutagenesis using Phusion polymerase (Finnzymes, Finland). Primers sequences are available upon request. All mutants were sequence verified and cloned into pcDNA5-EF1α-IRES-Zeo.

Cell lines

The murine fibroblast cell lines NIH 3T3 clone 2.2 and HER14 were described previously (Honegger et al., 1987). The tumor cell line UM-SCC-14C was kindly provided by G.A.M.S. van Dongen (Department of Otolaryngology, VU University Medical Center, Amsterdam, The Netherlands) and A431 and HeLa were both obtained from ATCC (LGC Standards, Germany). HeLa cells expressing a temperature-sensitive variant of the dynamin-K44A mutant were described previously and were kindly provided by Willem Stoorvogel (Department of Veterinary medicine, Utrecht University, Utrecht, The Netherlands) (Altschuler et al., 1998; Damke et al., 1995; van Dam and Stoorvogel, 2002). All cell lines were cultured as described previously (Roovers et al., 2011). Stable cell lines expressing the EGFR mutants were generated as described by Hofman et al. (Hofman et al., 2010). Zeocin-resistant cells were FACS-sorted for comparable EGFR levels as HER14 cells (3×10^5 receptors/cell (Honegger et al., 1987)).

Immunofluorescence

Immunofluorescence was performed as described previously (Stoorvoge et al., 2004). $EGF^{Alexa488}$, $Trf^{Alexa546}$, $CTB^{Alexa546}$ and Alexa Fluor 488 5-TFP were obtained from Invitrogen. In case of the alcohol treatments, cells were pretreated with 1% 1-butanol or 2-propanol for 1 minute before the assay. Images were obtained using a Zeiss Axiovert 200M confocal microscope (Carl Zeiss Microscopy GmbH, Germany) equipped with a 63× water-immersion objective (NA 1.2) or a Zeiss LSM700 confocal microscope (Carl Zeiss Microscopy GmbH, Germany) with a 63× oil-immersion objective (NA 1.4). The Pearson colocalization coefficient was determined using the ZEN 2011 software.

Homo-FRET anisotropy measurements

A detailed description of our confocal anisotropy imaging setup and homo-FRET method was published previously (Bader et al., 2007; Bader et al., 2009; Hofman et al., 2010). Briefly, a 473 nm solid-state diode laser (Becker and Hickl, BDL-473-SMC) with a pulse repetition rate of 80 MHz polarized by a linear polarizer (Meadowlark, Frederick, CO) was coupled into a confocal microscope (Nikon C1, Japan). The laser light is focused on sample by a 60× water-immersion objective (1.2 N.A., Nikon). Depolarization of excitation light due to high NA of the objective was reduced by under-filling its back aperture. Since the pinhole is located in the emission path only, the resolution was not affected. The emission is detected by a 515/30 nm band-pass filter and a broadband polarizing beam-splitter cube (PBS, OptoSigma, Santa Ana, CA) was used to split the emission in a parallel and a perpendicular channel with respect to the excitation light. The signal was detected with two high quantum efficiency PMTs (Hamamatsu H7422P-40). Calibration of the system was preformed with GFP in 50/50 glycerol/buffer and an aqueous Fluorescein solution.

^{125}I-labeling and internalization

VHHs and EGF were labeled according to the IODO-GEN method, as described by Salacinski et al. (Salacinski et al., 1981). Internalization assays using ^{125}I-labeled protein were performed as described before (Wiley and Cunningham, 1982). Radioactivity of both surface bound fraction and internalized fraction were determined using the gamma counter and the ratio internalized:bound was plotted against time to determine specific internalization rate constants.

TIRF-M

Live-cell imaging by dual-color total internal reflection fluorescence microscopy (TIRF-M) was performed on an inverted microscope (Eclipse Ti-E, Nikon) with a Perfect Focus System (Nikon), equipped with an Apo CFI Apo TIRF 100× /1.49 NA oil objective (Nikon). The system was also equipped with a stage-top incubator (INUG2E-ZILCS, Tokai Hit) and cells were imaged in the Phenol-Red-Free culture medium (Gibco) at 37℃ and 5% CO_2. For excitation, a mercury lamp HBO-103W/2 (Osram) or 491 nm 100 mW Calypso (Cobolt) and 561 nm 100 mW Jive (Cobolt) lasers were used. Emitted light was separated using an OptoSplit III image splitter (CAIRN Research Ltd, UK) equipped with an eGFP/mCherry filter cube (59022, Chroma). Movies were collected for up to 50 seconds (10 frames/second), using a Photometrics Evolve 512 Back-illuminated EMCCD camera (Roper Scientific) that was controlled by MetaMorph 7.7.5 software (Molecular Devices). The 16-bit images were projected onto the CCD chip with intermediate 2.5× lens at a magnification of 0.063 μm/pixel.

RNA interference

Small-interfering RNA (siRNA) knockdown was performed as described by Motley et al. (Motley et al., 2003). The siRNAs against CHC, AP2 alpha subunit, and a scrambled negative control were adapted from Motley et al. (Motley et al., 2003) or Fallon et al. (Fallon et al., 2006) and obtained as Stealth® siRNAs from Invitrogen. The following siRNAs were used: 5′-CCAUCUUCUUAAC-CCUGAGUGGUUA-3′ for clathrin heavy chain (CHC; starting from nucleotide 252), 5′-CCUGGAGAGCAUGUGCACGCUGGCC-3′ for the alpha subunit of the AP2 complex, 5′-AACAAACAAGAAUUCUUUGUUGCUU-3′ for Eps15/Eps15R and 5′-CCUUGACGUCAUAGUCAUUUGUGGA-3′ as a scrambled negative control. Knockdown efficiency was checked on a blot with antibodies against CHC (BD Biosciences), AP2 alpha (Sigma-Aldrich) and Eps15 (RF99, Schumacher et al., 1995). Dynasore was obtained from Sigma-Aldrich and used as described previously (Kirchhausen et al., 2008).

Downregulation and phosphorylation assays

Phosphorylation assays were performed by western blotting as described elsewhere (Roovers et al., 2007a). Phosphorylation of EGFR and total EGFR was checked with anti-pEGFR (Tyr 1068) (Cell Signaling Technology, Danvers, Massachusetts) anti-EGFR (c74B9, Cell Signaling Technology) antibodies, respectively. MAPK and phospho-MAPK was respectively checked with anti-MAP Kinase 2/Erk2 (1B3B9, Millipore Corporation, Bedford, Massachusetts) and anti-phospho-p44/42 MAPK (Erk1/2) (Thr202/Tyr204) (Cell Signaling Technology). Equal loading was checked with anti-actin (ICN Immunobiologicals, Irvine, CA) or anti-tubulin (DM1A, Millipore). Antibody binding to blots was detected with IRDye680- and IRDye800-conjugated secondary antibodies (LI-COR Biosciences, Lincoln, NE) and an Odyssey Infrared Imager (LI-COR Biosciences). EGF degradation was determined with ^{125}I-labeled EGF. Cells were pulsed with EGF in DMEM with 2% BSA, after which the medium was refreshed. After 4 hours at 37℃, the amount of free label in the medium was determined after protein precipitation in 10% TCA. Degraded EGF was plotted as the percentage free label compared with the total EGF uptake.

Acknowledgements

We would like to thank Casper Hoogenraad, Anna Akhmanova and Ilya Grigoriev for their support. Ger Arkesteijn is acknowledged for his help with the cell sorting and Cilia de Heus, Rachid El Khoulati,

Wang Li Ching, Mohamed Kaplan and Nivard Kagie for their contribution to this work.

Author contributions

R.H. and P.v.B.e.H. have designed the study. R.H., J.F.V., J.V. and R.C.R. performed the cell biological experiments. F.F., A.B. and H.C. performed the anisotropy experiments. All authors read, revised and approved the manuscript.

Funding

This study was funded by the Focus & Massa project of the Utrecht University, The Netherlands, and by a grant from arGEN-X, Ghent, Belgium.

Supplementary material available online at
http://jcs.biologists.org/lookup/suppl/doi:10.1242/jcs.128611/-/DC1

References

Altschuler, Y., Barbas, S. M., Terlecky, L. J., Tang, K., Hardy, S., Mostov, K. E. and Schmid, S. L. (1998). Redundant and distinct functions for dynamin-1 and dynamin-2 isoforms. *J. Cell Biol.* **143**, 1871-1881.

Ariotti, N., Liang, H., Xu, Y., Zhang, Y., Yonekubo, Y., Inder, K., Du, G., Parton, R. G., Hancock, J. F. and Plowman, S. J. (2010). Epidermal growth factor receptor activation remodels the plasma membrane lipid environment to induce nanocluster formation. *Mol. Cell. Biol.* **30**, 3795-3804.

Bader, A. N., Hofman, E. G., van Bergen En Henegouwen, P. M. and Gerritsen, H. C. (2007). Imaging of protein cluster sizes by means of confocal time-gated fluorescence anisotropy microscopy. *Opt. Express* **15**, 6934-6945.

Bader, A. N., Hofman, E. G., Voortman, J., en Henegouwen, P. M. and Gerritsen, H. C. (2009). Homo-FRET imaging enables quantification of protein cluster sizes with subcellular resolution. *Biophys. J.* **97**, 2613-2622.

Bader, A. N., Hoetzl, S., Hofman, E. G., Voortman, J., van Bergen en Henegouwen, P. M., van Meer, G. and Gerritsen, H. C. (2011). Homo-FRET imaging as a tool to quantify protein and lipid clustering. *ChemPhysChem* **12**, 475-483.

Benmerah, A., Bayrou, M., Cerf-Bensussan, N. and Dautry-Varsat, A. (1999). Inhibition of clathrin-coated pit assembly by an Eps15 mutant. *J. Cell Sci.* **112**, 1303-1311.

Berger, C., Madshus, I. H. and Stang, E. (2012). Cetuximab in combination with anti-human IgG antibodies efficiently down-regulates the EGF receptor by macropinocytosis. *Exp. Cell Res.* **318**, 2578-2591.

Berkers, J. A., van Bergen en Henegouwen, P. M. and Boonstra, J. (1991). Three classes of epidermal growth factor receptors on HeLa cells. *J. Biol. Chem.* **266**, 922-927.

Boersma, Y. L., Chao, G., Steiner, D., Wittrup, K. D. and Plückthun, A. (2011). Bispecific designed ankyrin repeat proteins (DARPins) targeting epidermal growth factor receptor inhibit A431 cell proliferation and receptor recycling. *J. Biol. Chem.* **286**, 41273-41285.

Boucrot, E., Saffarian, S., Massol, R., Kirchhausen, T. and Ehrlich, M. (2006). Role of lipids and actin in the formation of clathrin-coated pits. *Exp. Cell Res.* **312**, 4036-4048.

Burgess, A. W. (2008). EGFR family: structure physiology signalling and therapeutic targets. *Growth Factors* **26**, 263-274.

Citri, A. and Yarden, Y. (2006). EGF-ERBB signalling: towards the systems level. *Nat. Rev. Mol. Cell Biol.* **7**, 505-516.

Clayton, A. H., Walker, F., Orchard, S. G., Henderson, C., Fuchs, D., Rothacker, J., Nice, E. C. and Burgess, A. W. (2005). Ligand-induced dimer-tetramer transition during the activation of the cell surface epidermal growth factor receptor-A multidimensional microscopy analysis. *J. Biol. Chem.* **280**, 30392-30399.

Clayton, A. H., Tavarnesi, M. L. and Johns, T. G. (2007). Unligated epidermal growth factor receptor forms higher order oligomers within microclusters on A431 cells that are sensitive to tyrosine kinase inhibitor binding. *Biochemistry* **46**, 4589-4597.

Clayton, A. H., Orchard, S. G., Nice, E. C., Posner, R. G. and Burgess, A. W. (2008). Predominance of activated EGFR higher-order oligomers on the cell surface. *Growth Factors* **26**, 316-324.

Cymer, F. and Schneider, D. (2010). Transmembrane helix-helix interactions involved in ErbB receptor signaling. *Cell Adh. Migr.* **4**, 299-312.

Damke, H., Baba, T., Warnock, D. E. and Schmid, S. L. (1994). Induction of mutant dynamin specifically blocks endocytic coated vesicle formation. *J. Cell Biol.* **127**, 915-934.

Damke, H., Baba, T., van der Bliek, A. M. and Schmid, S. L. (1995). Clathrin-independent pinocytosis is induced in cells overexpressing a temperature-sensitive mutant of dynamin. *J. Cell Biol.* **131**, 69-80.

Endres, N. F., Das, R., Smith, A. W., Arkhipov, A., Kovacs, E., Huang, Y., Pelton, J. G., Shan, Y., Shaw, D. E., Wemmer, D. E. et al. (2013). Conformational coupling across the plasma membrane in activation of the EGF receptor. *Cell* **152**, 543-556.

Escher, C., Cymer, F. and Schneider, D. (2009). Two GxxxG-like motifs facilitate promiscuous interactions of the human ErbB transmembrane domains. *J. Mol. Biol.* **389**, 10-16.

Fallon, L., Belanger, C. M., Corera, A. T., Kontogiannea, M., Regan-Klapisz, E., Moreau, F., Voortman, J., Haber, M., Rouleau, G, Thorarinsdottir, T. et al. (2006). A regulated interaction with the UIM protein Eps15 implicates parkin in EGF receptor trafficking and PI(3)K-akt signalling. *Nat. Cell Biol.* **8**, 834-842.

Friedman, L. M., Rinon, A., Schechter, B., Lyass, L., Lavi, S., Bacus, S. S., Sela, M. and Yarden, Y. (2005). Synergistic down-regulation of receptor tyrosine kinases by combinations of mAbs: implications for cancer immunotherapy. *Proc. Natl. Acad. Sci. USA* **102**, 1915-1920.

Garrett, T. P., McKern, N. M., Lou, M., Elleman, T. C., Adams, T. E., Lovrecz, G. O., Zhu, H. J., Walker, F., Frenkel, M. J., Hoyne, P. A. et al. (2002). Crystal structure of a truncated epidermal growth factor receptor extracellular domain bound to transforming growth factor alpha. *Cell* **110**, 763-773.

Goh, L. K., Huang, F., Kim, W., Gygi, S. and Sorkin, A. (2010). Multiple mechanisms collectively regulate clathrin-mediated endocytosis of the epidermal growth factor receptor. *J. Cell Biol.* **189**, 871-883.

Groenen, L. C., Walker, F., Burgess, A. W. and Treutlein, H. R. (1997). A model for the activation of the epidermal growth factor receptor kinase involvement of an asymmetric dimer? *Biochemistry* **36**, 3826-3836.

Hackel, B. J., Neil, J. R., White, F. M. and Wittrup, K. D. (2012). Epidermal growth factor receptor downregulation by small heterodimeric binding proteins. *Protein Eng. Des. Sel.* **25**, 47-57.

Haigler, H., Ash, J. F., Singer, S. J. and Cohen, S. (1978). Visualization by fluorescence of the binding and internalization of epidermal growth factor in human carcinoma cells A-431. *Proc. Natl. Acad. Sci. USA* **75**, 3317-3321.

Heisermann, G. J. and Gill, G. N. (1988). Epidermal growth factor receptor threonine and serine residues phosphorylated in vivo. *J. Biol. Chem.* **263**, 13152-13158.

Henne, W. M., Boucrot, E., Meinecke, M., Evergren, E., Vallis, Y., Mittal, R. and McMahon, H. T. (2010). FCHo proteins are nucleators of clathrin-mediated endocytosis. *Science* **328**, 1281-1284.

Herbst, J. J., Opresko, L. K., Walsh, B. J., Lauffenburger, D. A. and Wiley, H. S. (1994). Regulation of postendocytic trafficking of the epidermal growth factor receptor through endosomal retention. *J. Biol. Chem.* **269**, 12865-12873.

Hofman, E. G., Ruonala, M. O., Bader, A. N., van den Heuvel, D., Voortman, J., Roovers, R. C., Verkleij, A. J., Gerritsen, H. C. and van Bergen En Henegouwen, P. M. (2008). EGF induces coalescence of different lipid rafts. *J. Cell Sci.* **121**, 2519-2528.

Hofman, E. G., Bader, A. N., Voortman, J., van den Heuvel, D. J., Sigismund, S., Verkleij, A. J., Gerritsen, H. C. and van Bergen en Henegouwen, P. M. (2010). Ligand-induced EGF receptor oligomerization is kinase-dependent and enhances internalization. *J. Biol. Chem.* **285**, 39481-39489.

Honegger, A. M., Szapary, D., Schmidt, A., Lyall, R., Van Obberghen, E., Dull, T. J., Ullrich, A. and Schlessinger, J. (1987). A mutant epidermal growth factor receptor with defective protein tyrosine kinase is unable to stimulate proto-oncogene expression and DNA synthesis. *Mol. Cell. Biol.* **7**, 4568-4571.

Huang, F., Jiang, X. and Sorkin, A. (2003). Tyrosine phosphorylation of the beta2 subunit of clathrin adaptor complex AP-2 reveals the role of a di-leucine motif in the epidermal growth factor receptor trafficking. *J. Biol. Chem.* **278**, 43411-43417.

Huang, F., Khvorova, A., Marshall, W. and Sorkin, A. (2004). Analysis of clathrin-mediated endocytosis of epidermal growth factor receptor by RNA interference. *J. Biol. Chem.* **279**, 16657-16661.

Huang, F., Goh, L. K. and Sorkin, A. (2007). EGF receptor ubiquitination is not necessary for its internalization. *Proc. Natl. Acad. Sci. USA* **104**, 16904-16909.

Jézéquel, P., Campion, L., Joalland, M. P., Millour, M., Dravet, F., Classe, J. M., Delecroix, V., Deporte, R., Fumoleau, P. and Ricolleau, G. (2004). G388R mutation of the FGFR4 gene is not relevant to breast cancer prognosis. *Br. J. Cancer* **90**, 189-193.

Jost, M., Simpson, F., Kavran, J. M., Lemmon, M. A. and Schmid, S. L. (1998). Phosphatidylinositol-4,5-bisphosphate is required for endocytic coated vesicle formation. *Curr. Biol.* **8**, 1399-1404.

Jura, N., Endres, N. F., Engel, K., Deindl, S., Das, R., Lamers, M. H., Wemmer, D. E., Zhang, X. and Kuriyan, J. (2009). Mechanism for activation of the EGF receptor catalytic domain by the juxtamembrane segment. *Cell* **137**, 1293-1307.

Kirchhausen, T., Macia, E. and Pelish, H. E. (2008). Use of dynasore, the small molecule inhibitor of dynamin, in the regulation of endocytosis. *Methods Enzymol.* **438**, 77-93.

Lai, W. H., Cameron, P. H., Wada, I., Doherty, J. J., I. I, Kay, D. G., Posner, B. I. and Bergeron, J. J. (1989). Ligand-mediated internalization, recycling, and downregulation of the epidermal growth factor receptor in vivo. *J. Cell Biol.* **109**, 2741-2749.

Li, E. and Hristova, K. (2006). Role of receptor tyrosine kinase transmembrane domains in cell signaling and human pathologies. *Biochemistry* **45**, 6241-6251.

Liu, A. P., Aguet, F., Danuser, G. and Schmid, S. L. (2010). Local clustering of transferrin receptors promotes clathrin-coated pit initiation. *J. Cell Biol.* **191**, 1381-1393.

Lu, C., Mi, L. Z., Grey, M. J., Zhu, J., Graef, E., Yokoyama, S. and Springer, T. A. (2010). Structural evidence for loose linkage between ligand binding and kinase activation in the epidermal growth factor receptor. *Mol. Cell. Biol.* **30**, 5432-5443.

MacKenzie, K. R., Prestegard, J. H. and Engelman, D. M. (1997). A transmembrane helix dimer: structure and implications. *Science* **276**, 131-133.

Madshus, I. H. and Stang, E. (2009). Internalization and intracellular sorting of the EGF receptor: a model for understanding the mechanisms of receptor trafficking. *J. Cell Sci.* **122**, 3433-3439.

Mendrola, J. M., Berger, M. B., King, M. C. and Lemmon, M. A. (2002). The single transmembrane domains of ErbB receptors self-associate in cell membranes. *J. Biol. Chem.* **277**, 4704-4712.

Mineev, K. S., Bocharov, E. V., Pustovalova, Y. E., Bocharova, O. V., Chupin, V. V. and Arseniev, A. S. (2010). Spatial structure of the transmembrane domain heterodimer of ErbB1 and ErbB2 receptor tyrosine kinases. *J. Mol. Biol.* **400**, 231-243.

Monsonego-Ornan, E., Adar, R., Feferman, T., Segev, O. and Yayon, A. (2000). The transmembrane mutation G380R in fibroblast growth factor receptor 3 uncouples ligand-mediated receptor activation from down-regulation. *Mol. Cell. Biol.* **20**, 516-522.

Motley, A., Bright, N. A., Seaman, M. N. and Robinson, M. S. (2003). Clathrin-mediated endocytosis in AP-2-depleted cells. *J. Cell Biol.* **162**, 909-918.

Muyldermans, S., Atarhouch, T., Saldanha, J., Barbosa, J. A. and Hamers, R. (1994). Sequence and structure of VH domain from naturally occurring camel heavy chain immunoglobulins lacking light chains. *Protein Eng.* **7**, 1129-1135.

Pines, G., Köstler, W. J. and Yarden, Y. (2010). Oncogenic mutant forms of EGFR: lessons in signal transduction and targets for cancer therapy. *FEBS Lett.* **584**, 2699-2706.

Polo, S. and Di Fiore, P. P. (2006). Endocytosis conducts the cell signaling orchestra. *Cell* **124**, 897-900.

Rappoport, J. Z. and Simon, S. M. (2009). Endocytic trafficking of activated EGFR is AP-2 dependent and occurs through preformed clathrin spots. *J. Cell Sci.* **122**, 1301-1305.

Roovers, R. C., Laeremans, T., Huang, L., De Taeye, S., Verkleij, A. J., Revets, H., de Haard, H. J. and van Bergen en Henegouwen, P. M. (2007a). Efficient inhibition of EGFR signaling and of tumour growth by antagonistic anti-EFGR nanobodies. *Cancer Immunol. Immunother.* **56**, 303-317.

Roovers, R. C., van Dongen, G. A. and van Bergen en Henegouwen, P. M. (2007b). Nanobodies in therapeutic applications. *Curr. Opin. Mol. Ther.* **9**, 327-335.

Roovers, R. C., Vosjan, M. J., Laeremans, T., el Khoulati, R., de Bruin, R. C., Ferguson, K. M., Verkleij, A. J., van Dongen, G. A. and van Bergen en Henegouwen, P. M. (2011). A biparatopic anti-EGFR nanobody efficiently inhibits solid tumour growth. *Int. J. Cancer* **129**, 2013-2024.

Saffarian, S., Li, Y., Elson, E. L. and Pike, L. J. (2007). Oligomerization of the EGF receptor investigated by live cell fluorescence intensity distribution analysis. *Biophys. J.* **93**, 1021-1031.

Salacinski, P. R., McLean, C., Sykes, J. E., Clement-Jones, V. V. and Lowry, P. J. (1981). Iodination of proteins, glycoproteins, and peptides using a solid-phase oxidizing agent, 1,3,4,6-tetrachloro-3 alpha,6 alpha-diphenyl glycoluril (Iodogen). *Anal. Biochem.* **117**, 136-146.

Schmitz, K. R., Bagchi, A., Roovers, R. C., van Bergen En Henegouwen, P. M. and Ferguson, K. M. (2013). Structural evaluation of EGFR inhibition mechanisms for Nanobodies/VHH domains. *Structure* **21**, 1214-1224.

Schumacher, C., Knudsen, B. S., Ohuchi, T., Di Fiore, P. P., Glassman, R. H. and Hanafusa, H. (1995). The SH3 domain of crk binds specifically to a conserved proline-rich motif in Eps15 and Eps15R. *J. Biol. Chem.* **270**, 15341-15347.

Sigismund, S., Woelk, T., Puri, C., Maspero, E., Tacchetti, C., Transidico, P., Di Fiore, P. P. and Polo, S. (2005). Clathrin-independent endocytosis of ubiquitinated cargos. *Proc. Natl. Acad. Sci. USA* **102**, 2760-2765.

Sorkin, A. and Goh, L. K. (2008). Endocytosis and intracellular trafficking of ErbBs. *Exp. Cell Res.* **314**, 3093-3106.

Spangler, J. B., Neil, J. R., Abramovitch, S., Yarden, Y., White, F. M., Lauffenburger, D. A. and Wittrup, K. D. (2010). Combination antibody treatment down-regulates epidermal growth factor receptor by inhibiting endosomal recycling. *Proc. Natl. Acad. Sci. USA* **107**, 13252-13257.

Sternberg, M. J. and Gullick, W. J. (1989). Neu receptor dimerization. *Nature* **339**, 587.

Sternberg, M. J. and Gullick, W. J. (1990). A sequence motif in the transmembrane region of growth factor receptors with tyrosine kinase activity mediates dimerization. *Protein Eng.* **3**, 245-248.

Sunada, H., Magun, B. E., Mendelsohn, J. and MacLeod, C. L. (1986). Monoclonal antibody against epidermal growth factor receptor is internalized without stimulating receptor phosphorylation. *Proc. Natl. Acad. Sci. USA* **83**, 3825-3829.

Thiel, K. W. and Carpenter, G. (2007). Epidermal growth factor receptor juxtamembrane region regulates allosteric tyrosine kinase activation. *Proc. Natl. Acad. Sci. USA* **104**, 19238-19243.

Van Bockstaele, F., Holz, J. B. and Revets, H. (2009). The development of nanobodies for therapeutic applications. *Curr. Opin. Investig. Drugs* **10**, 1212-1224.

van Dam, E. M. and Stoorvogel, W. (2002). Dynamin-dependent transferrin receptor recycling by endosome-derived clathrin-coated vesicles. *Mol. Biol. Cell* **13**, 169-182.

Wang, Q., Zhu, F. and Wang, Z. (2007). Identification of EGF receptor C-terminal sequences 1005-1017 and di-leucine motif 1010LL1011 as essential in EGF receptor endocytosis. *Exp. Cell Res.* **313**, 3349-3363.

Whitson, K. B., Beechem, J. M., Beth, A. H. and Staros, J. V. (2004). Preparation and characterization of Alexa Fluor 594-labeled epidermal growth factor for fluorescence resonance energy transfer studies: application to the epidermal growth factor receptor. *Anal. Biochem.* **324**, 227-236.

Wiley, H. S. and Cunningham, D. D. (1982). The endocytotic rate constant. A cellular parameter for quantitating receptor-mediated endocytosis. *J. Biol. Chem.* **257**, 4222-4229.

Wiley, H. S. (2003). Trafficking of the ErbB receptors and its influence on signaling. *Exp. Cell Res.* **284**, 78-88.

Yarden, Y. (2001). The EGFR family and its ligands in human cancer. signalling mechanisms and therapeutic opportunities. *Eur. J. Cancer* **37 Suppl. 4**, S3-S8.

Supplemental Movies and Figures

Movie S1. Internalization of EGF via a clathrin-coated pit.
Internalization of EGF-Alexa488 (green) was analyzed in HER14 cells expressing mRFP-clathrin (red). Movie was collected in TIRF mode for 30 sec at 10 frames/sec. Bar is 1µm.

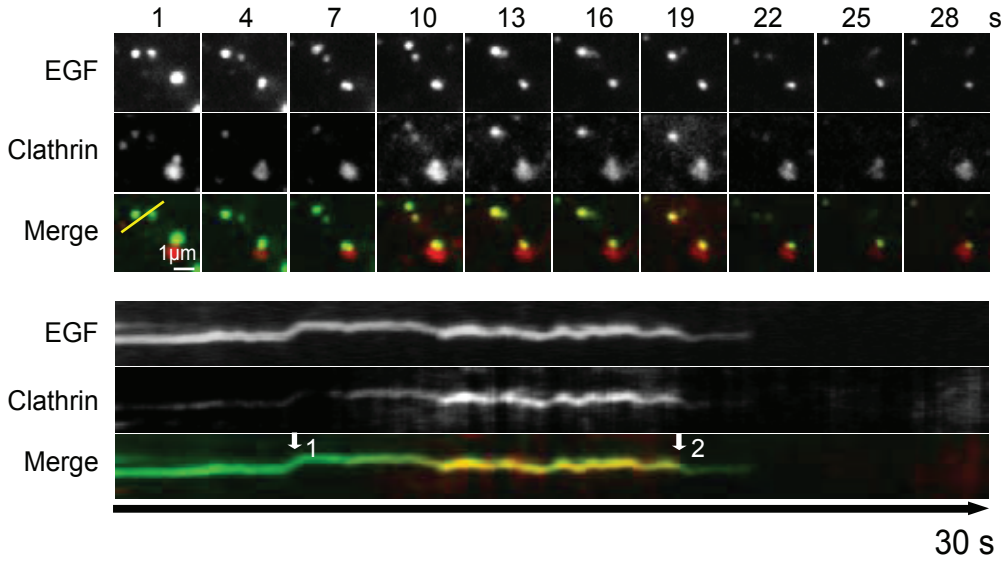

Figure S1. Analysis of EGF internalization via coated pit.
Screen shots of TIRF-M Movie 1 showing internalization of EGF. The bottom panel shows the kymographs of the indicated area (yellow line) generated for both channels separately and merged. Kymographs were generated using MetaMorph 7.7.5 software (Molecular Devices). Arrow 1 indicates colocalization of EGF with clathrin and arrow 2 indicates pinching off from the plasma membrane.

Movie 2. Internalization of Bipar1 via a clathrin-coated pit.
Internalization of Bipar1-Alexa488 (green) was analyzed in HER14 cells expressing mRFP-clathrin (red). Movie was collected in TIRF mode for 50 sec at 10 frames/sec. Bar is 1µm.

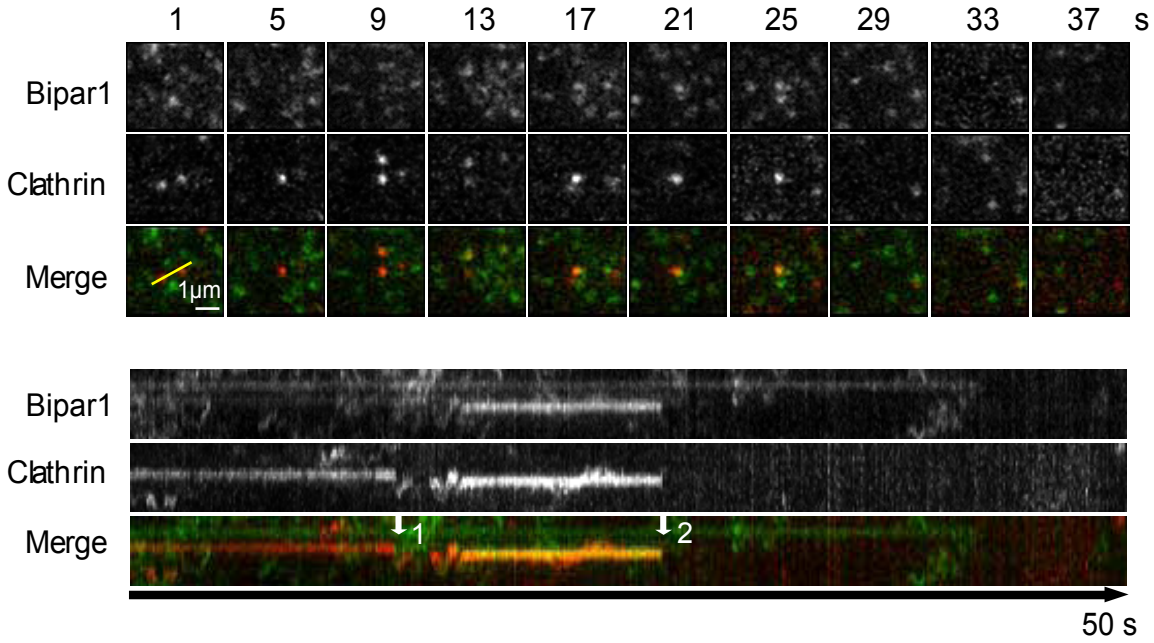

Figure S2. Analysis of Bipar1 internalization via coated pit.
Screen shots of TIRF-M Movie2 showing internalization of Bipar1. The bottom panel shows the kymographs of the indicated area (yellow line) generated for both channels separately and merged. Kymographs were generated using MetaMorph 7.7.5 software (Molecular Devices).

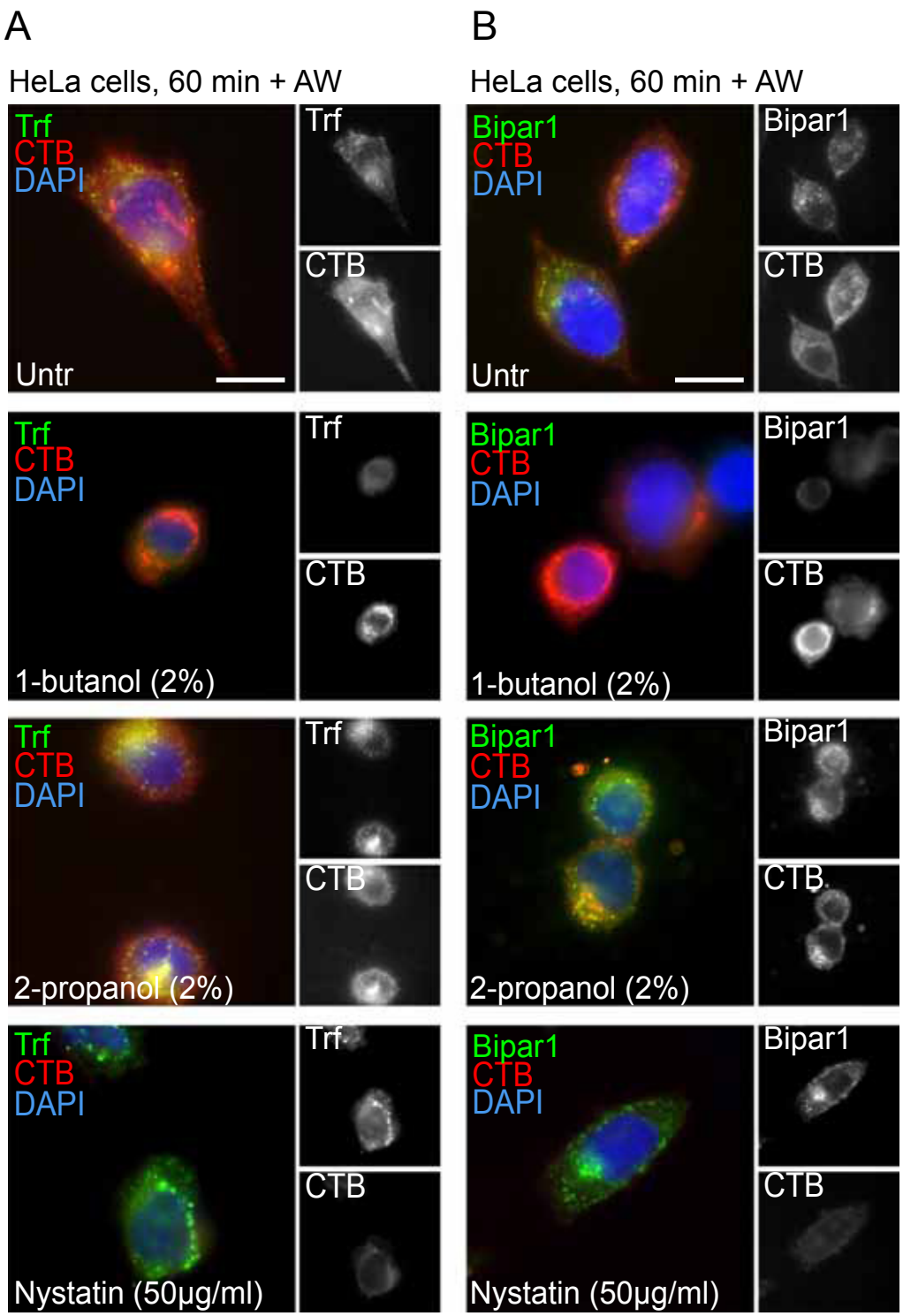

Figure S3. Bipar1 internalization is dependent on PIP2 but independent of caveolin. PIP2 production and thereby clathrin-mediated endocytosis was blocked by pre-treatment with 2% 1-butanol for 2 min. As controls, cells were either left untreated or were treated with 2% 2-propanol. For inhibition of caveolin-mediated endocytosis, 14C cells were pre-treated with 50 µg/ml Nystatin for 2 min. Bipar1-Alexa488 or Transferrin-Alexa488 (Trf) were prebound together with Cholera toxin B-Alexa555 (CTB) to cells on ice and were allowed to internalize in the presence of 1-butanol, 2-propanol or Nystatin for 60 min. Bound ligands were removed by acid wash and cells were fixed in 4% PFA. Bar is 15 µm.

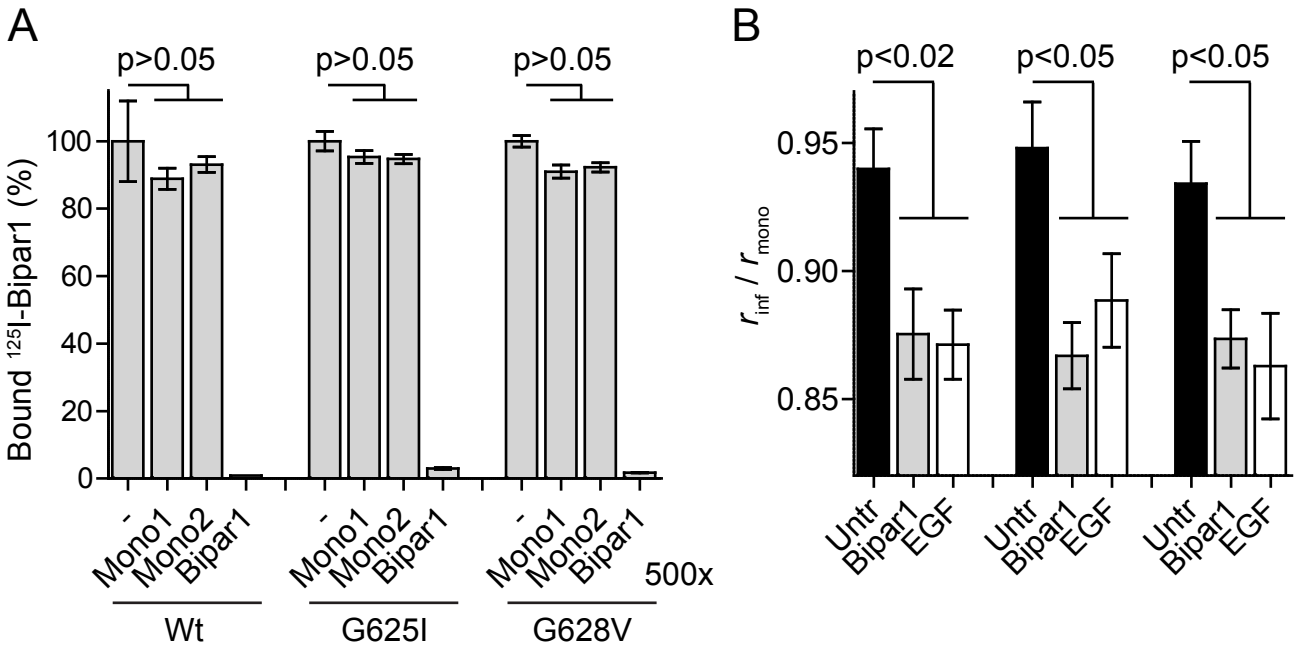

Figure S4. Bipar1 and EGF induces clustering of EGFR TMD mutants.
A. Bipar1 binds to EGFR TMD mutants with both epitope-binding domains. ^{125}I-Bipar1 with or without a 500x excess of unlabeled Mono1, Mono2 or Bipar1 was allowed to bind cells stably expressing EGFR wt or the TMD mutants for 2h on ice. Note that competition is only obtained with excess Bipar1.**B.** Both Bipar1 and EGF induce clustering of EGFR TMD mutants. Cells expressing mGFP-tagged EGFR wt or TMD mutants were incubated with 10 nM of Bipar1 for 20 min and subsequently fixed in 4% PFA. The limiting average anisotropy (r_{inf}) was determined as described in the Materials and methods and was plotted as fraction of the anisotropy value of mGFP (r_{mono}). Error bars represent SEM with n>5.

Tabel S1

	molecules/cell	SD
HER14	2.7E+05	7.3E+03
LALA	1.8E+05	3.9E+04
1-653 LALA	3.2E+05	6.6E+03
K721A LALA	1.3E+05	2.6E+03
9Y LALA	1.0E+05	7.6E+03
G625I	2.8E+05	6.1E+03
1-653 G625I	3.9E+05	8.5E+03
K721A G625I	5.8E+05	1.1E+05
9Y G625I	2.3E+05	1.0E+04
G628V	5.4E+05	3.2E+04
1-653 G628V	4.2E+05	1.6E+04
K721A G628V	5.1E+05	1.3E+04
9Y G628V	2.5E+05	6.9E+03